



AFRL-RX-TY-TR-2008-4572

ADVANCED SPALL REPAIR METHODS AND EQUIPMENT

**Michael I. Hammons
Air Force Research Laboratory**

FEBRUARY 2009

Final Report for 1 October 2007 – 31 December 2008

**DISTRIBUTION STATEMENT A: Approved for public release;
distribution unlimited.**

The use of the name or mark of any specific manufacturer, commercial product, commodity, or service in this publication does not imply endorsement by the Air Force.

**AIRBASE TECHNOLOGIES DIVISION
MATERIALS AND MANUFACTURING DIRECTORATE
AIR FORCE RESEARCH LABORATORY
AIR FORCE MATERIEL COMMAND
139 BARNES DRIVE, SUITE 2
TYNDALL AIR FORCE BASE, FL 32403-5323**

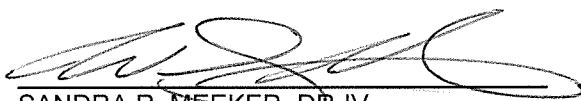
NOTICE AND SIGNATURE PAGE


Using Government drawings, specifications, or other data included in this document for any purpose other than Government procurement does not in any way obligate the U.S. Government. The fact that the Government formulated or supplied the drawings, specifications, or other data does not license the holder or any other person or corporation; or convey any rights or permission to manufacture, use, or sell any patented invention that may relate to them.

This report was cleared for public release by the Air Force Research Laboratory, Materials and Manufacturing Directorate, Airbase Technologies Division, Public Affairs and is available to the general public, including foreign nationals. Copies may be obtained from the Defense Technical Information Center (DTIC) (<http://www.dtic.mil>).

REPORT NUMBER AFRL-RX-TY-TR-2008-4572 HAS BEEN REVIEWED AND IS APPROVED FOR PUBLICATION IN ACCORDANCE WITH ASSIGNED DISTRIBUTION STATEMENT.



R. CRAIG MELLERSKI
Work Unit Manager

for SANDRA R. MEEKER, DR-IV
Chief, Deployed Base Systems Branch

ALBERT N. RHODES, PhD
Acting Chief, Airbase Technologies Division

This report is published in the interest of scientific and technical information exchange, and its publication does not constitute the Government's approval or disapproval of its ideas or findings.

REPORT DOCUMENTATION PAGE				<i>Form Approved</i> <i>OMB No. 0704-0188</i>	
The public reporting burden for this collection of information is estimated to average 1 hour per response, including the time for reviewing instructions, searching existing data sources, gathering and maintaining the data needed, and completing and reviewing the collection of information. Send comments regarding this burden estimate or any other aspect of this collection of information, including suggestions for reducing the burden, to Department of Defense, Washington Headquarters Services, Directorate for Information Operations and Reports (0704-0188), 1215 Jefferson Davis Highway, Suite 1204, Arlington, VA 22202-4302. Respondents should be aware that notwithstanding any other provision of law, no person shall be subject to any penalty for failing to comply with a collection of information if it does not display a currently valid OMB control number.					
PLEASE DO NOT RETURN YOUR FORM TO THE ABOVE ADDRESS.					
1. REPORT DATE (DD-MM-YYYY) 20-FEB-2009		2. REPORT TYPE Final Technical Report		3. DATES COVERED (From - To) 01-OCT-2007 -- 31-DEC-2008	
4. TITLE AND SUBTITLE Advanced Spall Repair Methods and Equipment				5a. CONTRACT NUMBER FA4819-07-D-0001	
				5b. GRANT NUMBER (Empty)	
				5c. PROGRAM ELEMENT NUMBER 62102F	
6. AUTHOR(S) Hammons, Michael I.				5d. PROJECT NUMBER 4915	
				5e. TASK NUMBER D1	
				5f. WORK UNIT NUMBER 4915D14B	
7. PERFORMING ORGANIZATION NAME(S) AND ADDRESS(ES) Air Force Research Laboratory, Materials and Manufacturing Directorate Airbase Technologies Division, Deployed Base Systems Branch 139 Barnes Drive, Suite 2 Tyndall Air Force Base, FL 32403-5323				8. PERFORMING ORGANIZATION REPORT NUMBER AFRL-RX-TY-TR-2008-4572	
9. SPONSORING/MONITORING AGENCY NAME(S) AND ADDRESS(ES) Headquarters Air Force Civil Engineer Support Agency 139 Barnes Drive, Suite 1 Tyndall Air Force Base, FL 32403-5323				10. SPONSOR/MONITOR'S ACRONYM(S) AFCESA	
				11. SPONSOR/MONITOR'S REPORT NUMBER(S) (Empty)	
12. DISTRIBUTION/AVAILABILITY STATEMENT Distribution Statement A: Approved for public release; distribution unlimited.					
13. SUPPLEMENTARY NOTES Ref AFRL/RXQ Public Affairs Case #09-041. Document contains color images.					
14. ABSTRACT <p>A series of experiments were performed using five excavation methods on nominal 2-foot wide, by 2-foot long by 4-inch deep spalls. The objective of this research was to develop one or more methods that will allow field personnel to excavate and prepare a 2-foot wide by 2-foot long by 4-inch deep spall for placement of a rapid-setting repair material in fifteen minutes or less. A secondary objective was to correlate various excavation methods with a relative life expectancy of the repair. Each of the methods tested had a significant improvement in production rate over the 30-pound jackhammer. The most efficient method was the cold planer, which, on average, was approximately 58 percent more efficient than the jackhammer.</p>					
15. SUBJECT TERMS pavement, spall repair, airfield damage repair, equipment					
16. SECURITY CLASSIFICATION OF:			17. LIMITATION OF ABSTRACT UU	18. NUMBER OF PAGES 62	19a. NAME OF RESPONSIBLE PERSON R. Craig Mellerski
a. REPORT U	b. ABSTRACT U	c. THIS PAGE U			19b. TELEPHONE NUMBER (Include area code) (Empty)

Reset

Table of Contents

Table of Contents.....	iii
List of Figures	v
List of Tables	vi
Summary	1
1 Introduction.....	3
1.1 Background.....	3
1.2 Objective.....	4
1.3 Scope.....	4
2 Experiment Description	6
2.1 Overview	6
2.2 Substrate Description.....	6
2.3 Excavation Equipment and Methods	6
2.3.1 30-lb Jackhammer.....	6
2.3.2 Hydraulic Breaker on Skid Steer Loader.....	8
2.3.3 Cold Planer	9
2.3.4 Gang Saw	11
2.4 Experiment Layout	13
2.5 Measures of Merit	14
2.5.1 Production Rate	14
2.5.2 Petrographic Examination.....	14
2.5.3 In-Situ Bond Strength.....	20
2.5.4 Direct Shear Strength	20
2.5.5 Performance under Simulated Aircraft Trafficking.....	20
2.6 Spall Repair Material	22
3 Experiment Results	24
3.1 Production Rate	24
3.2 Pre-Trafficking In-Situ Pull-Off Experiments.....	29
3.3 Pre-Trafficking Direct Shear Experiments.....	33
3.4 Simulated Aircraft Trafficking.....	37
3.5 Post-Trafficking In-Situ Pull-Off Experiments.....	37
3.6 Post-Trafficking Direct Shear Experiments	41
3.7 Petrographic Examination	44

3.7.1	Results.....	44
3.7.2	Analysis of Results	47
3.8	Summary of Significant Results	51
3.8.1	Production Rate	51
3.8.2	Bond Strength	51
3.8.3	Petrographic Examination.....	52
3.8.4	Performance under Traffic.....	52
4	Conclusions and Recommendations	53
4.1	Conclusions.....	53
4.1.1	Excavation Methods	53
4.1.2	Simulated Aircraft Trafficking.....	53
4.1.3	In-Situ Bond Strength.....	53
4.1.4	Direct Shear Strength	54
4.1.5	Petrographic Examination.....	54
4.2	Recommendations	54
5	References	55

List of Figures

1. 30-lb Jackhammer Used to Prepare Spalls.....	7
2. Photo of Completed Excavation using 30-lb Jackhammer.	8
3. Hydraulic Breaker on Wheeled Skid Steer Loader.....	9
4. Hole Excavated using Hydraulic Breaker.....	9
5. Cold Planer on Skid Steer Loader.....	10
6. Cold Planer Drum.	11
7. Excavations Prepared with Cold Planer.....	11
8. Multiple Blade Saw.....	12
9. Saw-cut Excavation (3/4-inch Spacing) Prior to Removal of Debris.	13
10. Saw-cut Excavation (3/4-inch Spacing) after Removal of Debris.....	13
11. Layout of Spall Locations before Excavation.....	14
12. URI System during Through-Transmission Scan.	15
13. 15 MHz Ultrasonic Transducer with a 1-inch Focal Distance used for Reflection Imaging.....	16
14. Autofeeding Concrete Saw and Polishing Wheel Used in Specimen Preparation.	17
15. Specimen on Turntable with Scanning Arm and Transmitting / Receiving Transducer (Tank is Dry).....	18
16. Process to Generate Scan Images from Focused Reflection Scan.	19
17. Example Data Showing Detection of Weak aggregate, Cracking, and Air Voids.	19
18. In-Situ Tensile Pull-off Test Preparation.....	21
19. Photograph of In-Situ Tensile Pull-off Test in Progress.....	21
20. Sketch of Direct Shear Test Device.	22
21. F-15E Load Cart.	22
22. Whisker Plot of Excavation Rate.....	27
23. P Value Matrix for Excavation Rate.....	27
24. Whisker Plot of Total Production Rate.....	28
25. P Value Matrix for Total Production Rate.....	28
26. Whisker Plot of Pre-Trafficking In-Situ Pull-Off Data.	32
27. P-Value Matrix for Pre-Trafficking In-Situ Pull-Off Experiments.	32
28. Whisker Plot of Pre-Trafficking Direct Shear Data.....	35
29. P Value Matrix for Pre-Trafficking Direct Shear Experiments.	35
30. Correlation of Pull-Off Strength and Direct Shear Strength.....	36
31. Whisker Plot of Post-Trafficking In-Situ Pull-Off Data.....	40
32. P Value Matrix for Post-Trafficking Direct Shear Experiments.	40
33. Whisker Plot of Post-Trafficking Direct Shear Data.	43
34. P Value Matrix for Post-Trafficking Direct Shear Experiments.	43
35. Raw Ultrasonic Reflection Image Data for Two Specimens Sets with One Duplicate Sample for Matching.....	44
36. Averaged Data in Z across Two Data Sets.	45
37. Color and Greyscale Images of First Group of Scanned Specimens.....	45
38. Color and Grayscale Images of the Second Group of Scanned Specimens.....	46
39. Adjustment of Ultrasonic Color Palette to Enhance Features.....	47

40. Images of Control Core.....	48
41. Images of Full Core from Pad.....	48
42. Images of Core from Gang Saw (1½-inch Spacing).....	49
43. Images of Core from Gang Saw (¾-inch Spacing).....	49
44. Images of Core from Cold Planer.	50
45. Images of Core from Jackhammer.	50
46. Images of Core from Hydraulic Breaker.	51

List of Tables

47. Rapid-Set Repair Material Properties.	23
48. Results of Production Rate Evaluations.....	26
49. Pre-trafficking In-Situ Pull-off Data.	29
50. Pre-trafficking Direct Shear Data.	34
51. Comparison between In-Situ Pull Strength and Direct Shear Strength.	36
52. Post-Trafficking In-situ Pull-Off Data.....	37
53. Post-Trafficking Direct Shear Data.	41
54. Figure and Specimen Relationship.	47

Summary

The objective of this research was to develop one or more methods that will allow field personnel to excavate and prepare a 2-foot-wide by 2-foot-long by 4-inch-deep spall for placement of a rapid-setting repair material in fifteen minutes or less. A secondary objective was to correlate various excavation methods with a relative life expectancy of the repair. The baseline method is to use a 30-pound jackhammer per AFCESA Engineering Technical Letter 07-08.

A series of experiments were performed using five excavation methods on nominal 2-foot-wide 2-foot-long by 4-inch-deep spalls:

1. Saw cut and 30-pound jackhammer (baseline or current standard),
2. Saw cut and a hydraulic breaker on a skid steer tractor,
3. Multiple-blade gang saw with saw spacing at $\frac{3}{4}$ inch,
4. Multiple-blade gang saw with saw spacing at $1\frac{1}{2}$ inches, and
5. Cold planer attachment for a skid steer loader.

Two measures of production rate were employed: 1) excavation production rate and 2) total production rate. In addition to the time required to repair (production rate), the repairs were evaluated to determine collateral damage and effects of the mechanical removal of the concrete. A petrographic exam was conducted to quantify any damage done to the substrate by the excavation method/equipment. The spall repairs were evaluated under 1500 passes of simulated F-15E traffic. Bond strength was evaluated by two methods: 1) in-situ tensile pull-off test and 2) a direct shear bond test.

Each of the methods tested had a significant improvement in production rate over the 30-pound jackhammer. The most efficient method was the cold planer, which, on average, was approximately 58 percent more efficient than the jackhammer. Only the cold planer can meet the requirement of being able to excavate 2-foot square by 4-inch deep spall in no more than 15 minutes.

The cold planer should be adopted as a standard method of preparing spalls for placement of a rapid-setting spall repair material. The cold planer equipment can be purchased as an attachment to skid-steer loaders. While the time to prepare a spall depends upon the characteristics of the spall and the skill of the operating, use of this equipment requires about half the time to prepare the spall as compared to the control case of a manual jackhammer. The cold planer equipment, under the control of an experienced operator, can prepare a two foot square by 4 inch deep spall for placement of rapid-setting material in less than 15 minutes. Furthermore, spalls prepared with this method retain superior bond strength after aircraft trafficking and are expected to provide superior performance compared to those

prepared with other conventional and experimental methods evaluated in the study.

1 Introduction

1.1 Background

A spall is described as cracking, breaking, chipping, or fraying of a concrete slab near a joint or crack. Spalls may be caused by one of more of the following mechanisms:

- Durability issues such as D-cracking and alkali-silica reaction (ASR);
- Inadequate maintenance, e.g., allowing foreign matter to collect in the joints;
- Improper construction procedures and details such as misaligned dowel bars, sawing joints too late, not sawing joints to adequate depth, or excessive working of the fresh concrete leading to a paste-rich mix;
- Fatigue caused by repeated mechanical loading of the joint by high-pressure aircraft tires; or
- Damage from munitions.

Spalls may be partial depth or full depth. In the case of both full- and partial-depth spalls, foreign object debris (FOD) may be generated, and rough surfaces at the spall may damage aircraft tires. Full-depth spalls reduce the structural capacity of the slab and exacerbate fatigue failure under repeated loading (1).

The normal procedure for repairing a spall is outlined in Engineering Technical Letter (ETL) 07-8 as follows (2):

- Remove loose debris from the damaged area.
- Mark the outer edge of the repair (2 to 3 inches beyond the damaged area).
- Saw the edges of the repair to a depth of at least 2 inches (50 millimeters). Do not feather the repair.
- Make additional cuts within the bounds of the repair edges using a concrete saw.
- Make transverse cuts on each end 1.5 inches (38 millimeters) from the ends of the repair.
- Remove the remaining material using a small jackhammer (30 pounds or less).
- Remove loose debris from the repair area.
- Wash the repair area with a high-pressure washer or use water and a scrub brush.
- Remove any loose material or lodged debris from the joint or crack.
- Place a small bead of caulk over the joint or crack.
- If using a cement-based repair material, soak the repair and leave saturated surface dry (SSD).
- Place a compressible insert material over any joint or crack in the repair area.

- Mix the materials in accordance with manufacturers' recommendations.
- A temperature gun (thermometer) should be used to check the temperature of the water and material before mixing, as well as the temperature of the material during mixing.
- Pour/place the material in the repair.
- Clean mixing and placement equipment immediately after use.
- When using cement repair materials, either wet cure or apply curing compound.
- Remove the compressible spacer insert after the repair has cured.
- Reseal the joint.

Because airfield operations are negatively impacted during the process of performing spall repairs, the time required to perform spall repairs is critical to maintaining the flying mission of the U.S. Air Force (USAF). The impact of the spall repair process on aircraft operations can vary by degree, ranging from an inconvenience to the complete suspension of flight operations.

The service life of a spall repair is dependent on many factors such as construction quality, repair material properties, and loading conditions. The most important factor is often the time required to construct a durable repair. As with any quick fix, there is often a tradeoff between expediency and quality. Expedient spall repairs are made when time, equipment, materials, and/or manpower are not available to perform a permanent repair. These extend the serviceability of a pavement using utilitarian methods, but durability and long-term performance may suffer as compared to permanent repair methods. Spall repairs at expeditionary locations have failed sooner than expected based upon accelerated pavement loading studies. Many of these repairs involve relatively non-uniformly shaped repairs that are loaded within a few hours after placement (3).

1.2 Objective

The objective of this research was to develop one or more methods that will allow field personnel to excavate and prepare a 2-foot-wide by 2-foot-long by 4-inch-deep spall for placement of a rapid-setting repair material in fifteen minutes or less. A secondary objective was to correlate various excavation methods with a relative life expectancy of the repair.

1.3 Scope

Selected equipment and procedures were evaluated to expeditiously prepare the spall for repair with rapid-setting materials. For five excavation methods, 2-foot-wide by 2-foot-long by 4-inch-deep spall were excavated in triplicate. The spalls were subsequently repaired using a typical rapid-setting spall repair material. The efficacy of the repair methods and equipment were evaluated based upon petrographic examination of the substrate excavation production rate, total production rate, in-situ tensile pull-off strength, direct shear bond strength, and

performance under simulated F-15 wheel loading. An optimal method was identified, and recommendations were proposed.

2 Experiment Description

2.1 Overview

A series of experiments were performed using five excavation methods (treatments) on nominal 2-foot-wide 2-foot-long by 4-inch-deep spalls:

1. Saw cut and 30-pound jackhammer (baseline or current standard),
2. Saw cut and a hydraulic breaker on a skid steer tractor,
3. Multiple-blade gang saw with saw spacing at $\frac{3}{4}$ inch,
4. Multiple-blade gang saw with saw spacing at $1\frac{1}{2}$ inches, and
5. Cold planer attachment for a skid steer loader.

After excavation, core samples were extracted from each treatment, and petrographic examinations were performed. Final preparation for each method consisted of pressure washing and excess water removal leaving the excavation clean and surface damp. The spalls were repaired with the same self-leveling cementitious repair material. A series of 2-inch-diameter cores were cut through the repair material and into the substrate. The cores were used to perform in-situ tensile pull-off tests to evaluate the bond between the repair material and the substrate. Also, a series of 4-inch diameter cores were cut, and direct shear tests were performed on the repair material/substrate interface. Finally, all spalls were trafficked for 1,500 passes using an F-15E load cart. The details of these experiments are presented in this chapter.

2.2 Substrate Description

All excavations were conducted on a jointed, unreinforced Portland cement concrete pavement at the 9700 Area at Tyndall AFB, FL. The pavement was approximately 20 years old at the time of the experiment. The pavement consisted of 10-ft square slabs approximately 12 inches thick and contained no dowel bars or other load transfer devices. The slabs were supported by a dense-graded limestone subbase which overlies a poorly graded (beach) sand subgrade. The aggregate in the concrete was crushed siliceous river gravel, and the compressive strength of the concrete averaged 8260 psi.

2.3 Excavation Equipment and Methods

2.3.1 30-lb Jackhammer

The common method to remove material from a spall repair is to use a portable pneumatic jackhammer as shown in Figure 1. ACI RAP Bulletin 7 recommends that jackhammers larger than 30 lbs not be used, because they may cause damage

to the surrounding concrete (4). For this experiment a 2 ft by 2 ft area was cut using a walk-behind saw to a depth of approximately 4 inches. The concrete inside the cut was removed with a 30-lb pneumatic jackhammer. A nail-point breaker tip was used to break up the concrete, and a spade tip was used to dress the repair area. Final clean up was performed by shoveling the rubble in to a loader bucket, sweeping around the hole, and vacuuming the fines from the hole. Figure 2 shows a photograph of a completed spall excavation prepared with the jackhammer.



Figure 1. 30-lb Jackhammer Used to Prepare Spalls.



Figure 2. Photo of Completed Excavation using 30-lb Jackhammer.

2.3.2 Hydraulic Breaker on Skid Steer Loader

The spall was prepared using a hydraulic percussion breaker fitted to a wheeled skid steer loader as shown in Figure 3. The breaker is powered by the auxiliary hydraulic system on the loader. The breaker had an operating weight of 736 lbs and produced 1310 blows per minute at a hydraulic flow rate of 17.2 gallons per minute yielding approximately 300 ft-lbs of impact energy. The diameter of the nail-type breaker probe was 2.56 inches.

Figure 4 contains a photograph of a completed spall excavation made with the hydraulic breaker.



Figure 3. Hydraulic Breaker on Wheeled Skid Steer Loader.



Figure 4. Hole Excavated using Hydraulic Breaker.

2.3.3 Cold Planer

Another set of holes was excavated using a Caterpillar Model PC206 Cold Planer powered by a CAT 257B high flow skid steer loader (Figure 5).

The hydraulic system on the loader was operated at the high setting (26 gallons per minute at 3,335 psi). The cold planer, designed for restoration of asphalt and concrete surfaces for small paving jobs, has a drum width of 24 inches. The drum (Figure 6) featured 60 carbide-tipped conical bits. The skid steer loader moves

backwards while lowering the drum in to the concrete. During the course of the excavation the cold planer depth adjustment was set to 4½ inches, because it appeared that the milling debris was precluding the planer from achieving its desired depth of 4 inches. Final clean up was performed with a shovel, broom, and shop vacuum.

Figure 7 shows a photograph of the completed excavations. Note that the cold planer drum leaves a radius in the excavation such that the bottom surface of the spall excavation is not parallel with the surface of the pavement.



Figure 5. Cold Planer on Skid Steer Loader.



Figure 6. Cold Planer Drum.



Figure 7. Excavations Prepared with Cold Planer.

2.3.4 Gang Saw

The final sets of excavations were performed using a prototype multiple-blade (gang) saw developed by Diamond Products.

Figure 8 shows a photograph of the gang saw. The total width of the saw blades was 24 inches. The saw consisted of a blade shaft with multiple 18-inch-diameter

diamond-tipped saw blades. The blade shaft was hydraulically driven by a Diamond Products CC8000 rider saw powered by a 78-hp diesel engine. The distance between the saw blades was variable, and two center-to-center spacings were employed ($\frac{3}{4}$ inch and $1\frac{1}{2}$ inches) for this research.

The saw was employed twice at right angles to produce an orthogonal grid of saw cuts. Three holes each were prepared with the saw blades spaced at $\frac{3}{4}$ inch or $1\frac{1}{2}$ inches. After the cuts were made, the material was removed with a 30-lb pneumatic jackhammer. Figure 9 and Figure 10 show photographs of the saw-cut excavations before and after removal of debris, respectively.



Figure 8. Multiple Blade Saw.



Figure 9. Saw-cut Excavation (3/4-inch Spacing) Prior to Removal of Debris.



Figure 10. Saw-cut Excavation (3/4-inch Spacing) after Removal of Debris.

2.4 Experiment Layout

As previously mentioned, the experiment consisted of trials on five excavation methods. Each excavation method was conducted in triplicate. Figure 11 shows a photograph of the layout of the 15 2-ft by 2-ft spall areas on the pavement prior to excavation. All spalls were required to have one (and only one) side along a joint.

The data recorded for each spall excavation were time to complete the excavation, time to complete clean out, and the volume of material removed. The volume of material removed was estimated by carefully measuring the volume of water required to fill the excavation.



Figure 11. Layout of Spall Locations before Excavation

2.5 Measures of Merit

The spall repair equipment and methods will be evaluated on the measures of merit described below.

2.5.1 Production Rate

Two measures of production rate were employed: 1) excavation production rate and 2) total production rate. The *excavation production rate* is defined as the time required to excavate the spall using the equipment and method evaluated. The *total production rate* is defined as the time required excavating 1 cu ft of spall, removing rubble, and preparing the spall repair for placement of rapid-setting repair material.

2.5.2 Petrographic Examination

One 6-inch-diameter core sample was removed from the interior of one excavation from each treatment (leaving two excavations from each treatment

intact). Additionally, one 6-inch-diameter core was extracted from the undamaged concrete around the excavation areas as a control. These samples were sent to the U. S. Army Engineer Research and Development Center (ERDC) at Vicksburg, Mississippi, where a petrographic exam was conducted to quantify any damage done to the substrate by the excavation method/equipment.

Ultrasonic reflection imaging (URI) was conducted on samples cored from the substrate materials after the excavation of the spalls was completed. The objective of the URI was to qualitatively identify levels of damage caused by various excavation techniques and to relate that to performance observed from the various mechanical testing results. The Concrete and Materials Division, Geotechnical and Structures Laboratory of the ERDC conducted the URI testing.

URI is a new technique for imaging concrete that focuses on the mechanical characteristics of the concrete paste and aggregate. It is particularly sensitive to locating damaged or weak aggregates, entrapped and/or entrained air, or failure between various interfaces. URI relies on a laboratory immersion scanning system to collect data from either smooth cored or cut concrete surfaces. The immersion scanning system is shown in Figure 12. Note that in this example a specimen (not from this project) is in the tank, and the tank is partially filled with water. The water serves to carry and focus the stress waves from the transducer to specimen face and back. The transducers used in this echo imaging effort are shown in Figure 13. Though not clear in this view, the front of the transducer is curved slightly to increase the focusing performance.

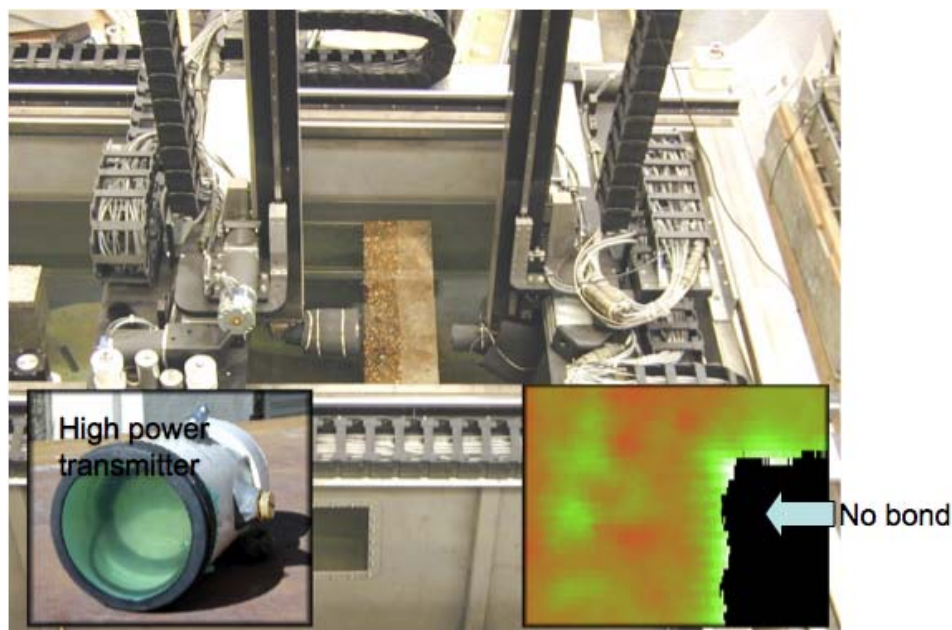


Figure 12. URI System during Through-Transmission Scan.



Figure 13. 15 MHz Ultrasonic Transducer with a 1-inch Focal Distance used for Reflection Imaging.

The immersion scanning system has eleven axes of motion control. The y- and z-axes were established on the exposed surfaces of the cores. A rotational axis was used in alignment of the y- and z-axes. The x-axis (normal to the y- and z-axes) was the distance from the specimen face to the transducer and was initially aligned for optimal focus. During the initial adjustment scanning ranges are set and tweaking is done to assure that the scanning plane is parallel to the specimen face throughout the test. The ultrasonic signal consists of a short broadband pulse. The amount of this focused pulse that gets reflected back at the transmitter / receiver is determined by the characteristic mechanical impedance of the media being targeted and the water. Snell law for normal incidence produces the derived relation below:

$$R \cong \left[\frac{(Z_2 - Z_1)}{(Z_2 + Z_1)} \right]^2$$

This relation describes the change in reflected energy by the material being targeted by the focused beam. If we assume our concrete impedance varies between 6 and 9 Megarayls ($10^6 \text{ kg}/(\text{m}^2 \text{ sec})$) then we would expect to see reflection coefficients varying between 0.36 and 0.5, respectively. For this example range we expect to see about 14 percent variation in reflected energy. In some more complex cases, such as small air voids and cracks, the energy is scattered differently either due to roughness (air voids) or additional mode conversion (microcracking).

Because very smooth surfaces are preferable for higher resolution effort our cores were cut in half and polished. Figure 14 shows the laboratory cutting and polishing equipment used in the processing of these specimens. The polished cores were scanned in two batches. One core was repeated in both scans to provide reference readings and validate comparable system operation.



Cutting



Polishing

Figure 14. Autofeeding Concrete Saw and Polishing Wheel Used in Specimen Preparation.

Figure 15 shows a group of cut and polished specimens sitting on the turntable in front of the scanning transducer. The water has been removed from the tank in this photograph. Scanning the specimens in groups help maintain scan to scan consistency in terms of the test setup and speeds up the overall process as alignment is a necessary and tedious part of the process. Either the turntable or vertical tilt is adjusted until the scanning plane of the transducer stays parallel with the face. The distance from transducer to specimen is measured on the personal computer that runs the scanning application as the two-way travel time or time of arrival of the pulse. Iteratively the axial alignments are adjusted until negligible changes in arrival times are observed. The multiple specimens are pre-set to be co-planar by placing them flat on a surface such as a tabletop (polished side down and using sulfur potting compound and/or quick set epoxy to grout the rounded surfaces together.



Figure 15. Specimen on Turntable with Scanning Arm and Transmitting / Receiving Transducer (Tank is Dry).

Figure 16 illustrates the measurement and data manipulation used to generate scans. In general the reflected pulse is digitized and the scan axis is indexed. After a line scan is completed the system moves the transducer back to the start location (one-direction scanning was done to minimize effects from system vibration) and collects the next line of data. Once the area has been scanned the amplitude data is color encoded and c-scan images are generated. Figure 17 shows a scan image where weak aggregates and cracks were imaged. Aggregate strength was verified by application of a scratch test.

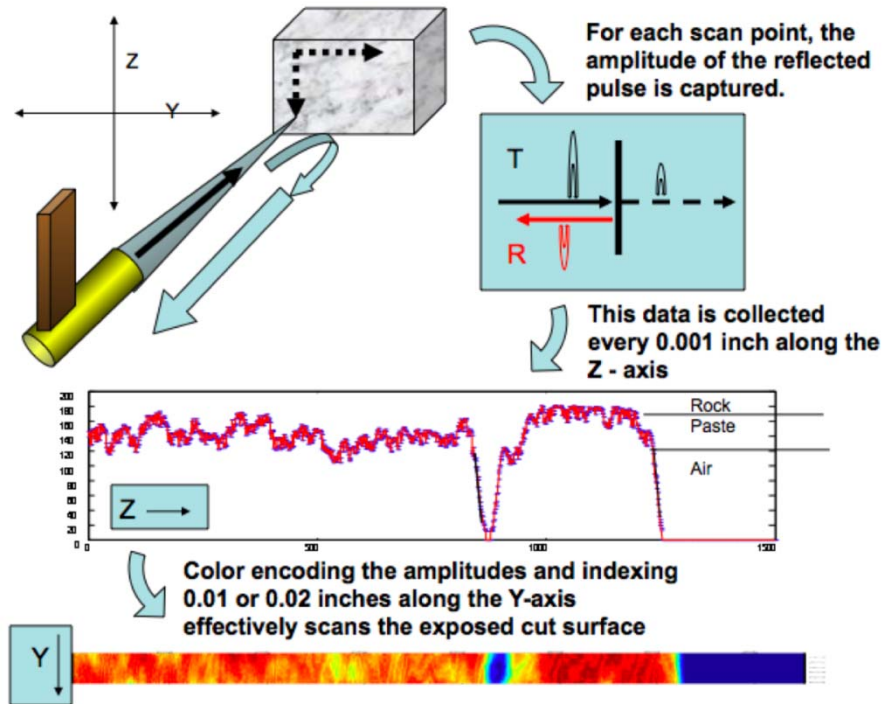


Figure 16. Process to Generate Scan Images from Focused Reflection Scan.

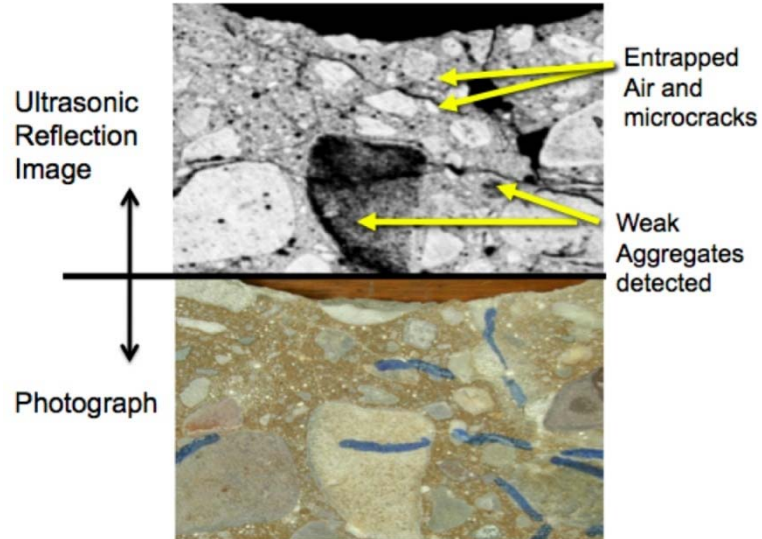


Figure 17. Example Data Showing Detection of Weak aggregate, Cracking, and Air Voids.

2.5.3 In-Situ Bond Strength

The in-situ tensile pull off test is described by the International Concrete Repair Guideline No. 03739 (5). This protocol, which is based upon ASTM D4541 (6), allows the user to evaluate the in-situ tensile bond strength.

Figure 18 shows a sketch of the test preparation. A core bit was used to drill through the repair material and into the substrate. A rigid disc was attached to the top of the drilled core using a high-strength adhesive. A testing device (Figure 19) applied a tensile force to the rigid disc at a constant rate until fracture occurred. The tensile force and location of the fracture (at the adhesive, at the bond interface, within the repair material, or within the substrate) were recorded.

2.5.4 Direct Shear Strength

An AFRL-developed testing protocol was employed to measure the direct shearing strength of the bond interface on 4-inch diameter cores extracted from the spall repairs. A direct shear test apparatus (as shown in the sketch in Figure 20) was fabricated in the shops at AFRL/RXQ. The apparatus consisted of two clamping yokes designed to secure the core to a base plate. A third yoke (or loading yoke) was positioned near the end of the core to transmit the shearing force to the core. Leather shims were employed to insure uniform contact between the core and the yokes at all contact areas. The apparatus and core were placed in a Forney Model LT-920-D2 universal testing machine capable of a maximum compressive force of 400,000 lbs, and the test was conducted at a loading rate of approximately 500 lbs/min. The load at fracture was recorded, and the shearing force at failure was calculated at the load at fracture divided by the cross-sectional area of the core.

2.5.5 Performance under Simulated Aircraft Trafficking

The spall repairs were evaluated under 1500 passes of AFRL's F-15E load cart (Figure 21). A single-lane trafficking pattern was used in which all tire loads were applied to the center of the spall repair area. One traverse of the spall field was defined as two passes (one pass up and one pass back). The wheel loading was 35,200 lbs. At 25, 50, 75, 100, and every 100 passes thereafter trafficking was paused, and the spall repairs were inspected and photographed. No active sensors or instrumentation were employed.

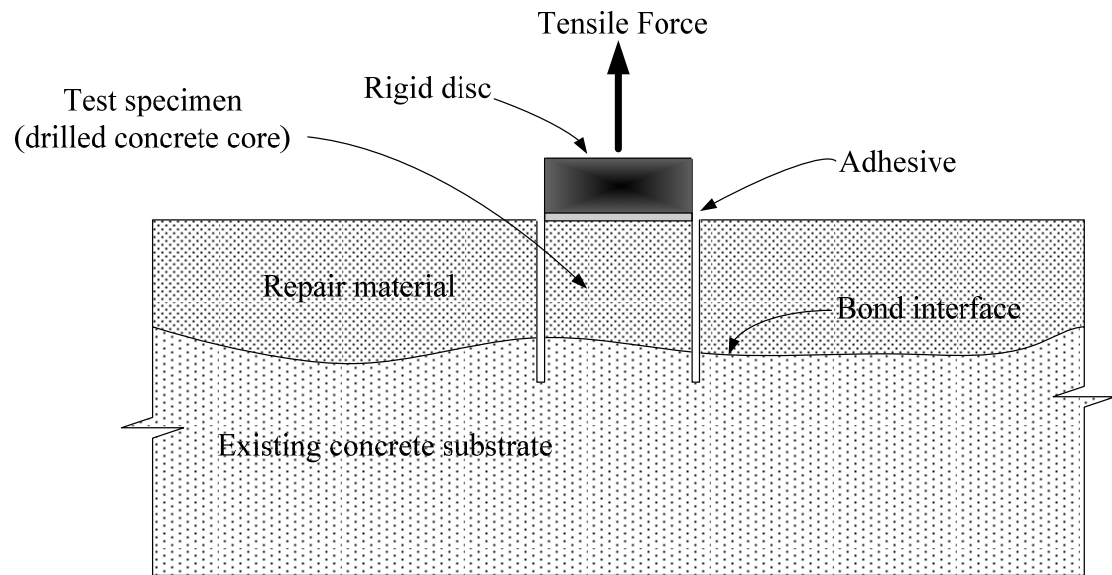


Figure 18. In-Situ Tensile Pull-off Test Preparation.



Figure 19. Photograph of In-Situ Tensile Pull-off Test in Progress.

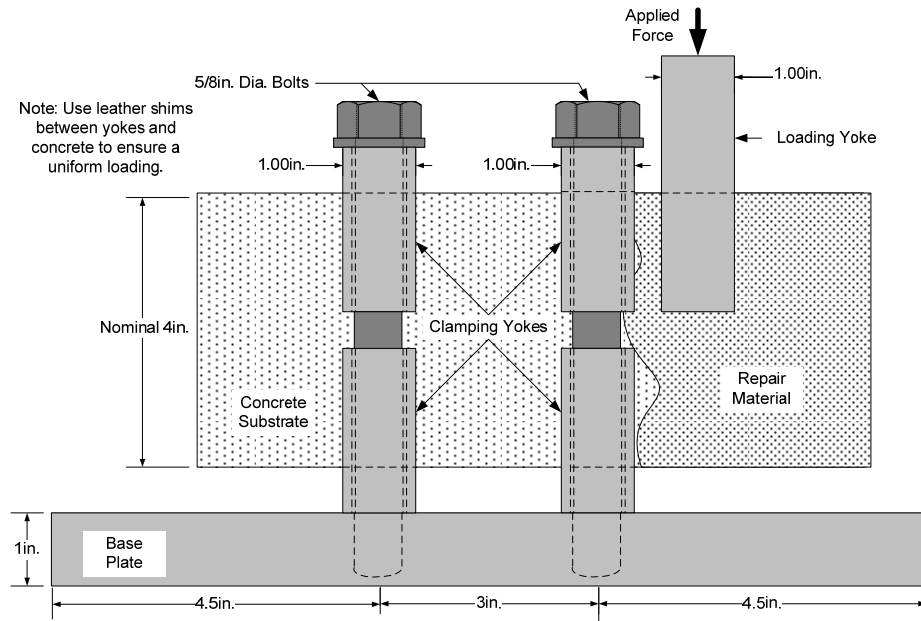


Figure 20. Sketch of Direct Shear Test Device.



Figure 21. F-15E Load Cart.

2.6 Spall Repair Material

A rapid-set spall repair material that has been tested at AFRL/RXQ for a related research project was selected for this study. It is a blend of propriety cements, ASTM concrete grade sand, air entrainment, and a high range water reducer. The manufacturer recommends its use for neat for applications from ½ to 4 inches

thick. The results of material properties tests conducted by AFRL are shown in Table 1.

Table 1. Rapid-Set Repair Material Properties.

<i>Age, hrs</i>	<i>Compressive Strength by ASTM C39, psi</i>	<i>Flexural Strength by ASTM C78, psi</i>	<i>Slant Shear Bond Strength by ASTM C 882, psi</i>
2	N/A	705	1120
3	4480	635	1170
24	6070	550	1220

3 Experiment Results

3.1 Production Rate

The times required to perform critical operations in spall repair preparations were observed and recorded for each trial and excavation method. As previously described, two measures of production rate were employed: 1) excavation production rate and 2) total production rate. The volume of each excavation was also documented by recording the volume of water required to rapidly fill each excavation. The production rate was then calculated by forming the ratio of the time required to the volume of the excavation in cubic feet, yielding a production rate in units of minutes/cubic feet. The results of these observations are presented in Table 2. The timing of operations started when the equipment first touched the pavement. The total production time included the time required to remove all debris and blow the area clean of any residual fine materials using compressed air.

The data in Table 2 were used to develop the plot shown in Figure 22, where the mean value of excavation rate is represented by the small squares, and the whisker bars represent ± 95 percent confidence intervals on the mean. There was considerable scatter in the data, as indicated by the length of the confidence intervals. Comparing only mean values of excavation rate revealed that the 30-lb jackhammer, the typical method of excavating spall repairs, was the least efficient method. The most efficient method was the cold planer, which, on average, was approximately 58 percent more efficient than the jackhammer. The second most efficient method was the hydraulic breaker, followed by gang saw with spacing at $1\frac{1}{2}$ inches and $\frac{3}{4}$ inch.

A pair wise t-test procedure was used to compare the means to determine if the observed differences in the mean value were statistically significant given the large scatter of the data. The results of these tests are presented in Figure 23. The value tabulated in each cell is the P value that resulted from the pair wise t-test for the combination of treatments represented by the cell. A lower P value indicates a greater significance. In Figure 23, all cells with a P value less than 0.05 are highlighted in orange. This indicates that there is a greater than 95 percent probability that the differences observed between the two methods are statistically significant. Using these analyses, we observe that the production rates for the 30-lb jackhammer are statistically different from those of the cold planer, hydraulic breaker, and the gang saw at $1\frac{1}{2}$ -inch spacing. Comparing with Figure 22, we observe that each of these methods is a significant improvement in production rate over the 30-lb jackhammer.

A similar analysis was performed for total production rate as illustrated in

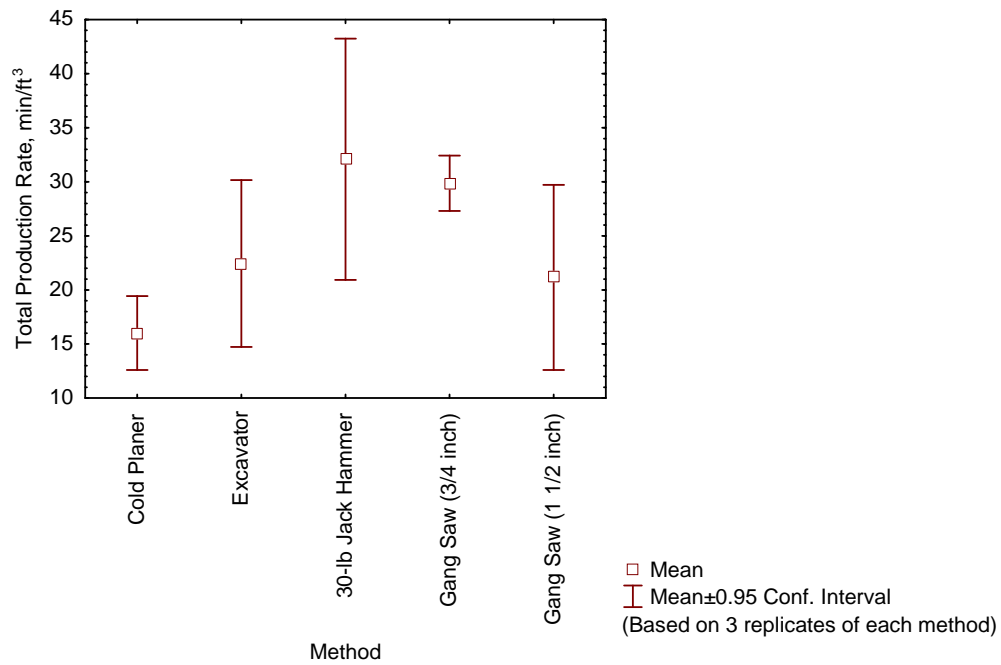


Figure 24 and Figure 25. The results were similar to that for excavation rate, except that the difference between the mean values for jackhammer method and the hydraulic breaker were significant in this case.

Table 2. Results of Production Rate Evaluations.

<i>Method Used</i>	<i>Trial Number</i>	<i>Nominal Surface Area, inches</i>	<i>Nominal Depth, inches</i>	<i>Volume Excavated, ft³†</i>	<i>Time Required for Excavation, min</i>	<i>Excavation Production Rate, min/ft³</i>	<i>Time Required to Remove Rubble, min</i>	<i>Total Production Rate, min/ft³</i>
Cold Planer	1-1 9700	23 by 24-1/4	4	0.78	10.58	13.56	13.44	17.23
Cold Planer	1-2 9700	24 by 24-1/4	3-3/4	0.99	11.62	11.74	14.37	14.52
Cold Planer	1-3 9700	24 by 23-1/2	3-1/2	0.74	9.08	12.27	12.04	16.27
Hydraulic Breaker	2-3 9700	23 by 24	4	1.13	21.50	19.03	26.00	23.01
Hydraulic Breaker	2-2 9700	23-1/2 by 23-1/2	4-1/4	1.06	16.00	15.09	20.25	19.10
Hydraulic Breaker	2-1 9700	26 by 25-1/2	5	1.45	34.35	23.69	36.60	25.24
30-lb Jackhammer	3-3 9700	24 by 24-3/4	4-1/4	1.27	42.20	33.23	45.20	35.59
30-lb Jackhammer	3-2 9700	23-1/4 by 23-3/4	4-3/4	1.24	31.00	25.00	33.50	27.02
30-lb Jackhammer	3-1 9700	23-3/4 by 23-1/2	4-1/4	1.13	34.50	30.53	38.00	33.63
Gang Saw (3/4 in.)	4-1 9700	27-3/4 by 25-1/4	4	1.13	31.37	27.76	35.03	31.00
Gang Saw (3/4 in.)	4-2 9700	27-3/4 by 25-1/4	3-3/4	1.27	33.85	26.65	37.60	29.61
Gang Saw (3/4 in.)	4-3 9700	26 by 25-1/4	4	1.09	29.80	27.34	31.60	28.99
Gang Saw (1-1/2 in.)	5-3 9700	21-1/2 by 24	3.5	0.92	14.88	16.17	21.80	23.70
Gang Saw (1-1/2 in.)	5-2 9700	24 by 24-1/2	3-3/4	1.13	13.73	12.15	19.48	17.24
Gang Saw (1-1/2 in.)	5-1 9700	24 by 24	3-5/8	1.06	18.48	17.43	23.90	22.55

† The excavation volume was not calculated from the nominal dimensions in this table. Rather, the volume was measured by observing the amount of water required to completely fill the excavation.

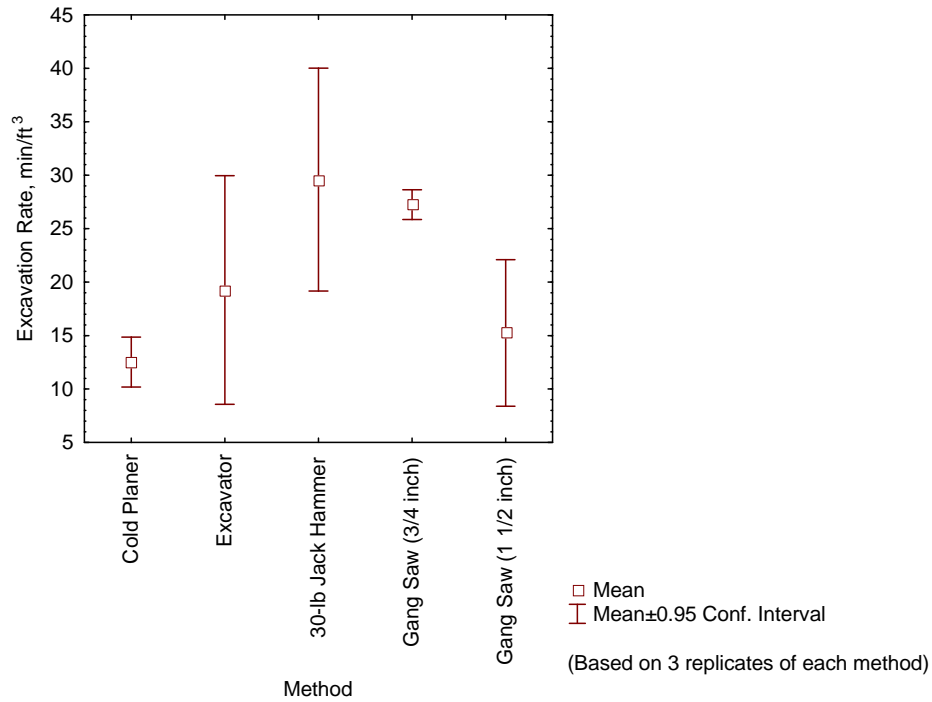


Figure 22. Whisker Plot of Excavation Rate.

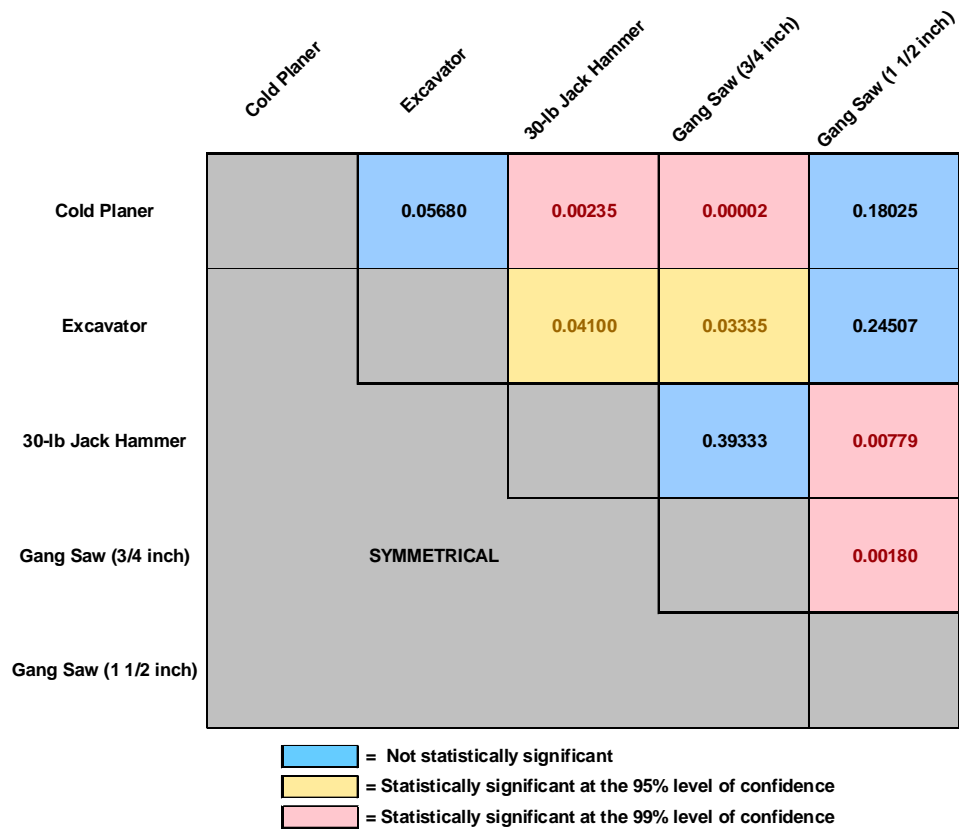


Figure 23. P Value Matrix for Excavation Rate.

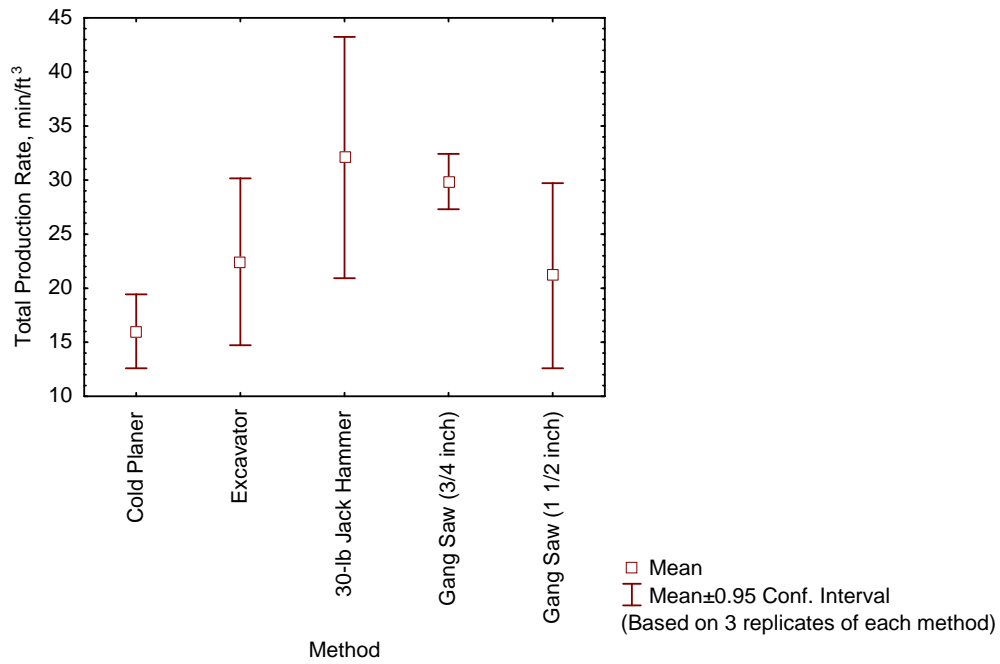


Figure 24. Whisker Plot of Total Production Rate.

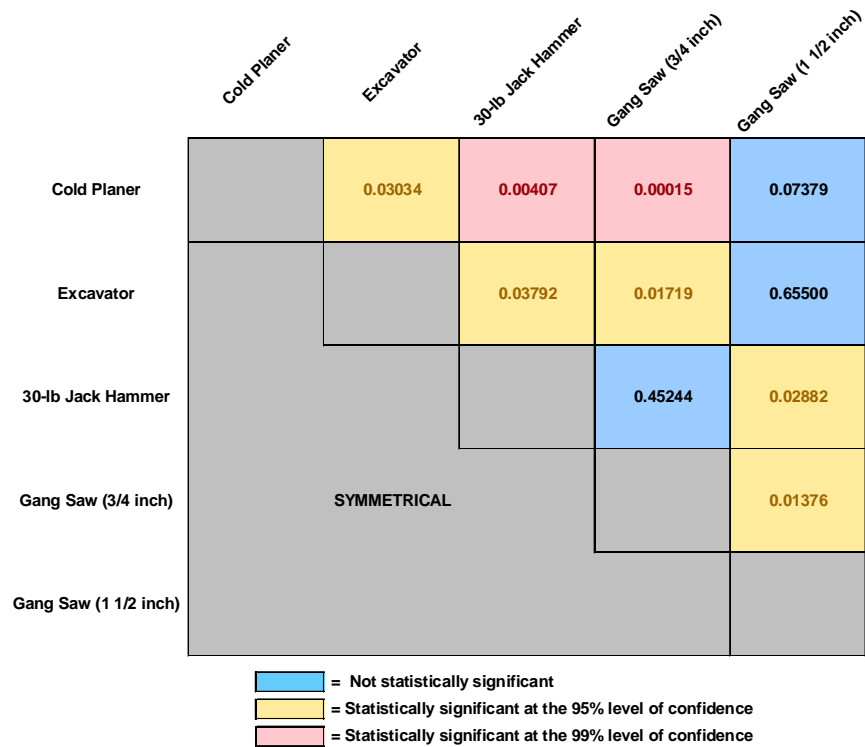


Figure 25. P Value Matrix for Total Production Rate.

3.2 Pre-Trafficking In-Situ Pull-Off Experiments

The results of the pre-trafficking in-situ pull-off experiments are tabulated in Table 3. The results are organized by the method, spall number, replicate number and pull-off strength. At the outset of the experiments, as many of the 2-inch-diameter cores were drilled as possible within the area allowed. A number of the cores were broken or became debonded during the coring process; therefore, number of replicates varied from spall-to-spall.

Table 3. Pre-trafficking In-Situ Pull-off Data.

<i>Trial</i>	<i>Method</i>	<i>Spall Number</i>	<i>Replicate</i>	<i>In-situ Pull-off Strength, psi</i>
1	Cold Planer	1-1	1	186
2	Cold Planer	1-2	1	18
3	Cold Planer	1-2	2	94
4	Cold Planer	1-2	3	130
5	Cold Planer	1-2	4	20
6	Cold Planer	1-2	5	286
7	Cold Planer	1-2	6	23
8	Cold Planer	1-3	1	121
9	Cold Planer	1-3	2	95
10	Cold Planer	1-3	3	202
11	Cold Planer	1-3	4	175
12	Cold Planer	1-3	5	135
13	Cold Planer	1-3	6	177
14	Hydraulic Breaker	2-1	1	86
15	Hydraulic Breaker	2-1	2	153
16	Hydraulic Breaker	2-1	3	240
17	Hydraulic Breaker	2-1	4	39
18	Hydraulic Breaker	2-1	5	218
19	Hydraulic Breaker	2-1	6	26
20	Hydraulic Breaker	2-1	7	77
21	Hydraulic Breaker	2-1	8	63
22	Hydraulic Breaker	2-1	9	142
23	Hydraulic Breaker	2-1	10	72
24	Hydraulic Breaker	2-1	11	81
25	Hydraulic Breaker	2-1	12	88
26	Hydraulic Breaker	2-2	1	152
27	Hydraulic Breaker	2-2	2	77
28	Hydraulic Breaker	2-2	3	69
29	Hydraulic Breaker	2-3	4	42
30	Hydraulic Breaker	2-3	5	54
31	Hydraulic Breaker	2-3	6	20
32	Hydraulic Breaker	2-3	7	31
33	Hydraulic Breaker	2-3	8	133
34	Hydraulic Breaker	2-3	9	24
35	Hydraulic Breaker	2-3	10	65
36	Hydraulic Breaker	2-3	11	64
37	Hydraulic Breaker	2-3	12	54

Table 3. Pre-trafficking In-Situ Pull-off Data (Continued).

<i>Trial</i>	<i>Method</i>	<i>Spall Number</i>	<i>Replicate</i>	<i>In-situ Pull-off Strength, psi</i>
38	Hydraulic Breaker	2-3	13	48
39	Jackhammer	3-1	1	200
40	Jackhammer	3-1	2	169
41	Jackhammer	3-1	3	184
42	Jackhammer	3-1	4	177
43	Jackhammer	3-1	5	103
44	Jackhammer	3-1	6	123
45	Jackhammer	3-1	7	284
46	Jackhammer	3-1	8	123
47	Jackhammer	3-1	9	135
48	Jackhammer	3-1	10	231
49	Jackhammer	3-1	11	24
50	Jackhammer	3-1	12	174
51	Jackhammer	3-1	13	234
52	Jackhammer	3-2	1	88
53	Jackhammer	3-2	2	34
54	Jackhammer	3-2	3	69
55	Jackhammer	3-2	4	36
56	Jackhammer	3-2	5	99
57	Jackhammer	3-2	6	57
58	Jackhammer	3-2	7	83
59	Jackhammer	3-2	8	36
60	Jackhammer	3-2	9	208
61	Jackhammer	3-2	10	98
62	Jackhammer	3-2	11	34
63	Jackhammer	3-2	12	218
64	Jackhammer	3-2	13	80
65	Jackhammer	3-3	1	20
66	Jackhammer	3-3	2	61
67	Gang Saw (3/4 in.)	4-1	1	73
68	Gang Saw (3/4 in.)	4-1	2	117
69	Gang Saw (3/4 in.)	4-1	3	43
70	Gang Saw (3/4 in.)	4-1	4	242
71	Gang Saw (3/4 in.)	4-1	5	115
72	Gang Saw (3/4 in.)	4-1	6	61
73	Gang Saw (3/4 in.)	4-1	7	10
74	Gang Saw (3/4 in.)	4-2	1	19
75	Gang Saw (3/4 in.)	4-2	2	145
76	Gang Saw (3/4 in.)	4-2	3	205
77	Gang Saw (3/4 in.)	4-2	4	101
78	Gang Saw (3/4 in.)	4-3	1	110
79	Gang Saw (3/4 in.)	4-3	2	33
80	Gang Saw (3/4 in.)	4-3	3	78
81	Gang Saw (3/4 in.)	4-3	4	24
82	Gang Saw (1-1/2 in.)	5-1	1	23
83	Gang Saw (1-1/2 in.)	5-1	2	198

Table 3. Pre-trafficking In-Situ Pull-off Data (Concluded).

<i>Trial</i>	<i>Method</i>	<i>Spall Number</i>	<i>Replicate</i>	<i>In-situ Pull-off Strength, psi</i>
84	Gang Saw (1-1/2 in.)	5-1	3	106
85	Gang Saw (1-1/2 in.)	5-1	4	176
86	Gang Saw (1-1/2 in.)	5-1	5	50
87	Gang Saw (1-1/2 in.)	5-1	6	156
88	Gang Saw (1-1/2 in.)	5-1	7	174
89	Gang Saw (1-1/2 in.)	5-1	8	269
90	Gang Saw (1-1/2 in.)	5-1	9	117
91	Gang Saw (1-1/2 in.)	5-1	10	157
92	Gang Saw (1-1/2 in.)	5-2	1	48
93	Gang Saw (1-1/2 in.)	5-2	2	52
94	Gang Saw (1-1/2 in.)	5-2	3	65
95	Gang Saw (1-1/2 in.)	5-2	4	4
96	Gang Saw (1-1/2 in.)	5-3	1	30
97	Gang Saw (1-1/2 in.)	5-3	2	69
98	Gang Saw (1-1/2 in.)	5-3	3	159
99	Gang Saw (1-1/2 in.)	5-3	4	129
100	Gang Saw (1-1/2 in.)	5-3	5	179
101	Gang Saw (1-1/2 in.)	5-3	6	31

The results of the pre-trafficking in-situ pull-off experiments are summarized in the plot shown in Figure 26. The greatest observed mean pull-off strength was for the cold planer, followed, in order, by the jackhammer, gang saw at 1½ inches spacing, gang saw at ¾ inch spacing, and finally the hydraulic breaker. However, the scatter in the data is quite large, and statistical analysis was required to evaluate the significance in the observed means. Pair wise t-tests were conducted on each of the observed treatments, and these results are summarized in Figure 27. The value tabulated in each cell is the P value that resulted from the pair wise t-test for the combination of treatments represented by the cell. A lower P value indicates a greater significance, and cells with a P value less than 0.05 are highlighted in orange. This indicates that there is a greater than 95 percent probability that the differences observed between the two methods are statistically significant. For these experiments, the t-tests indicated that only the differences in the means between the hydraulic breaker and cold planer and hydraulic breaker and jackhammer were statistically significant at the 95 percent confidence level, and one cannot statistically distinguish between the means of the other treatments at the 95 percent confidence level.

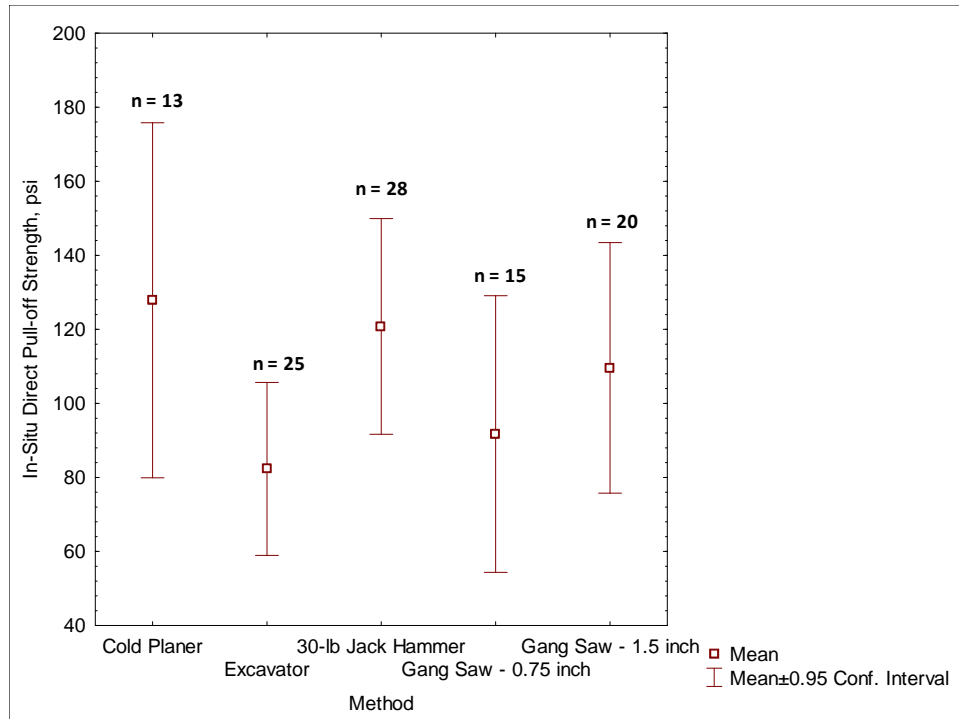


Figure 26. Whisker Plot of Pre-Trafficking In-Situ Pull-Off Data.

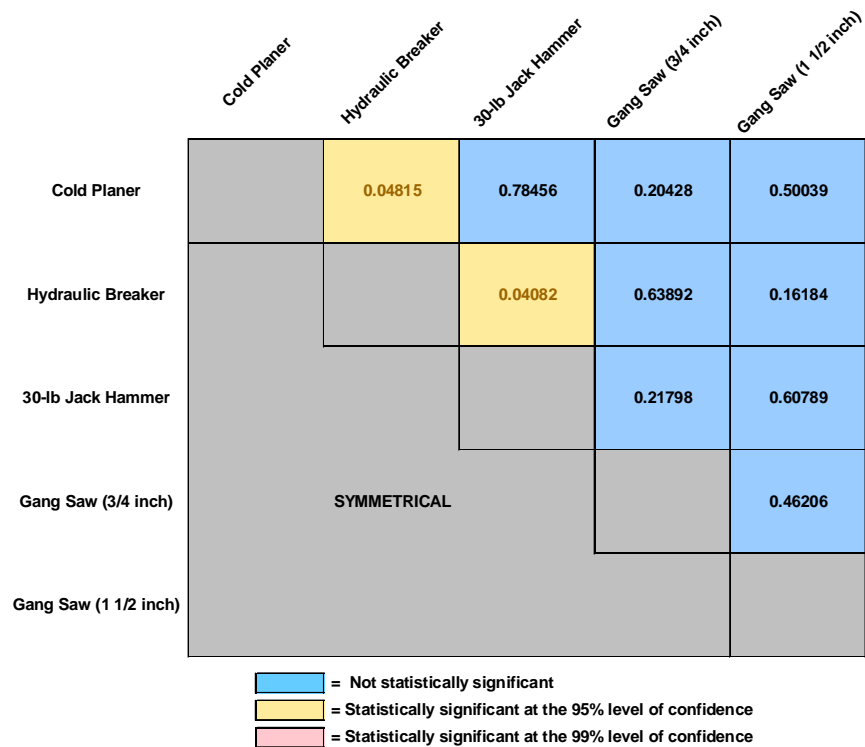


Figure 27. P-Value Matrix for Pre-Trafficking In-Situ Pull-Off Experiments.

3.3 Pre-Trafficking Direct Shear Experiments

The results of the pre-trafficking direct shear experiments are tabulated in Table 4. The results are organized by the method, spall number, replicate number and pull-off strength. The experiment plan was to obtain 4 replicates from each spall; however, some cores broke or became debonded during the coring operation. Most spalls produced three or four cores which could be evaluated in direct shear experiments.

The results of the pre-trafficking in-situ pull-off experiments are summarized in the plot shown in Figure 26. The greatest observed mean direct shear strength was for the cold planer, followed, in order, by the jackhammer, gang saw at 1½ inches spacing, gang saw at ¾ inch spacing, and finally the hydraulic breaker. However, once again, the scatter in the data is quite large, and statistical analysis was required to evaluate the significance in the observed means. Pair wise t-tests were conducted on each of the observed treatments, and these results are summarized in Figure 29. For these experiments, the t-tests indicated that only the differences in the means between the hydraulic breaker and jackhammer and gang saw were statistically significant at the 95 percent confidence level.

Table 5 summarizes the comparison between the in-situ tensile pull-off strength and the direct shear strength. A regression analysis was performed to determine the strength of the correlation between these two indications of bond strength. The results of this regression are shown in Figure 30. This analysis shows that the two metrics of bond strength are positively correlated with a correlation coefficient (R^2) of 0.66. These results indicate that both the in-situ tension pull-off test and direct shear test are indicators of the bond strength, with additional testing and numerical analysis required to improve the correlation between the two test methods.

Because the direct shear strength test is not an accepted test method per ASTM, the results of the direct shear strength tests will not be used to draw conclusions concerning the efficacy of the methods until further development and analysis of this testing methodology is conducted.

Table 4. Pre-trafficking Direct Shear Data.

<i>Trial</i>	<i>Method</i>	<i>Spall Number</i>	<i>Replicate</i>	<i>Direct Shear Strength, psi</i>
1	Cold Planer	1-1	1	108
2	Cold Planer	1-1	2	79
3	Cold Planer	1-1	3	348
4	Cold Planer	1-2	1	10
5	Cold Planer	1-2	2	247
6	Cold Planer	1-2	3	267
7	Cold Planer	1-3	1	86
8	Cold Planer	1-3	2	45
9	Cold Planer	1-3	3	91
10	Hydraulic Breaker	2-1	1	82
11	Hydraulic Breaker	2-1	2	109
12	Hydraulic Breaker	2-1	3	19
13	Hydraulic Breaker	2-1	4	70
14	Hydraulic Breaker	2-2	1	33
15	Hydraulic Breaker	2-2	2	92
16	Hydraulic Breaker	2-3	1	27
17	Hydraulic Breaker	2-3	2	55
18	30-lb Jackhammer	3-1	1	116
19	30-lb Jackhammer	3-1	2	228
20	30-lb Jackhammer	3-1	3	94
21	30-lb Jackhammer	3-1	4	161
22	30-lb Jackhammer	3-2	1	67
23	30-lb Jackhammer	3-2	2	72
24	30-lb Jackhammer	3-2	3	95
25	Gang Saw (3/4 in.)	4-1	1	144
26	Gang Saw (3/4 in.)	4-1	2	57
27	Gang Saw (3/4 in.)	4-1	3	176
28	Gang Saw (3/4 in.)	4-1	4	31
29	Gang Saw (3/4 in.)	4-2	1	58
30	Gang Saw (3/4 in.)	4-2	2	141
31	Gang Saw (3/4 in.)	4-3	1	83
32	Gang Saw (3/4 in.)	4-3	2	140
33	Gang Saw (3/4 in.)	4-3	3	207
34	Gang Saw (1-1/2 in.)	5-1	1	83
35	Gang Saw (1-1/2 in.)	5-1	2	59
36	Gang Saw (1-1/2 in.)	5-1	3	142
37	Gang Saw (1-1/2 in.)	5-1	4	55
38	Gang Saw (1-1/2 in.)	5-2	1	230
39	Gang Saw (1-1/2 in.)	5-2	2	168
40	Gang Saw (1-1/2 in.)	5-2	3	90
41	Gang Saw (1-1/2 in.)	5-2	4	154
42	Gang Saw (1-1/2 in.)	5-3	1	121

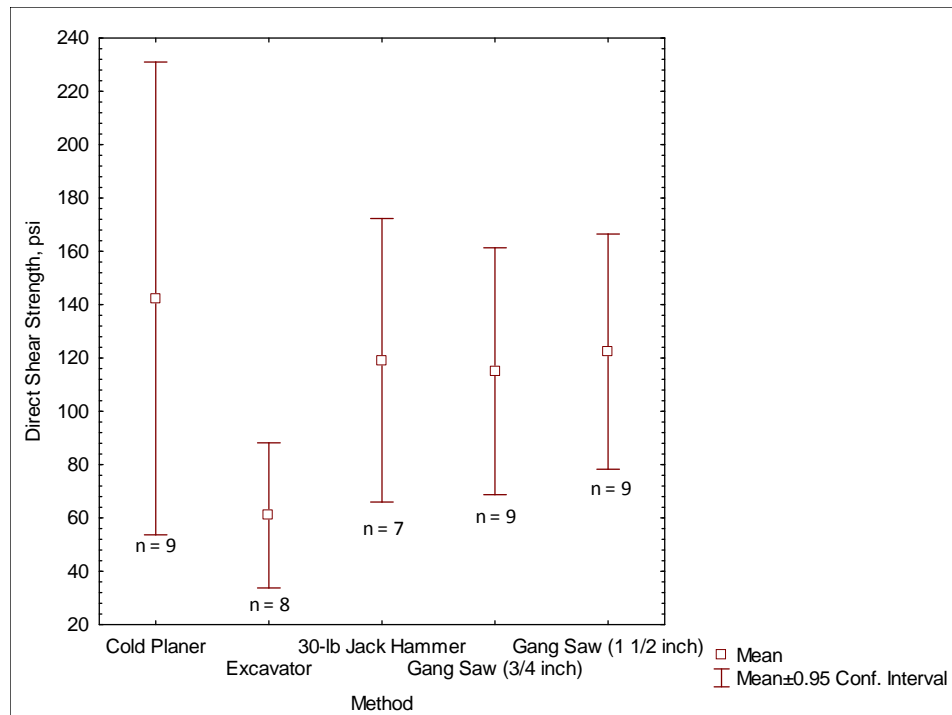


Figure 28. Whisker Plot of Pre-Trafficking Direct Shear Data.

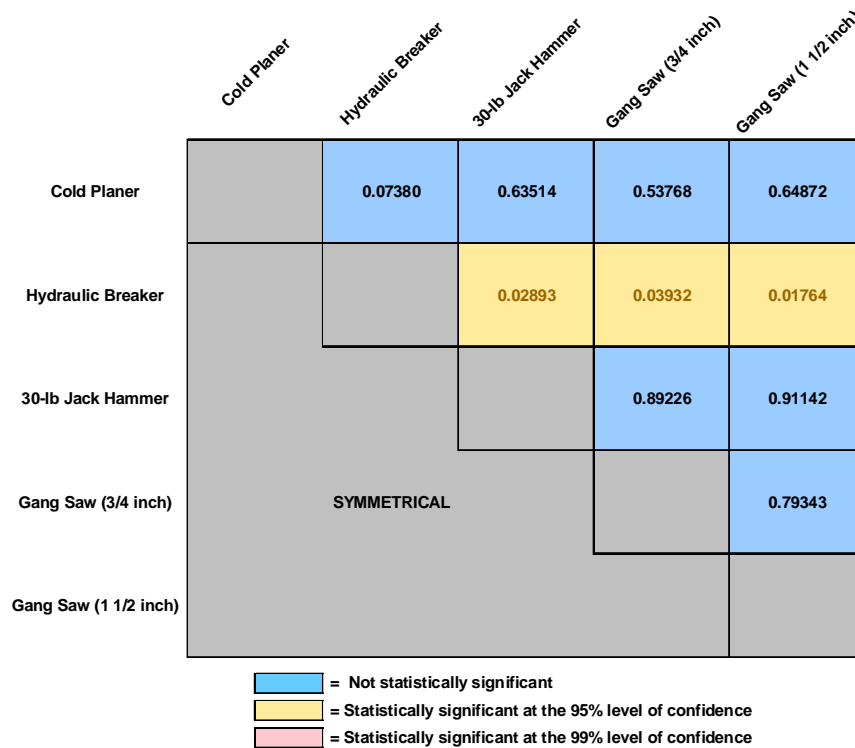


Figure 29. P Value Matrix for Pre-Trafficking Direct Shear Experiments.

Table 5. Comparison between In-Situ Pull Strength and Direct Shear Strength.

<i>Method</i>	<i>In-Situ Tensile Pull-off Grand Mean, psi</i>	<i>Direct Shear Grand Mean, psi</i>
Cold Planer	127.85	142.36
Hydraulic Breaker	82.31	52.02
30-lb Jackhammer	120.79	114.03
Gang Saw (3/4 in.)	91.73	114.77
Gang Saw (1½ in.)	109.60	122.05

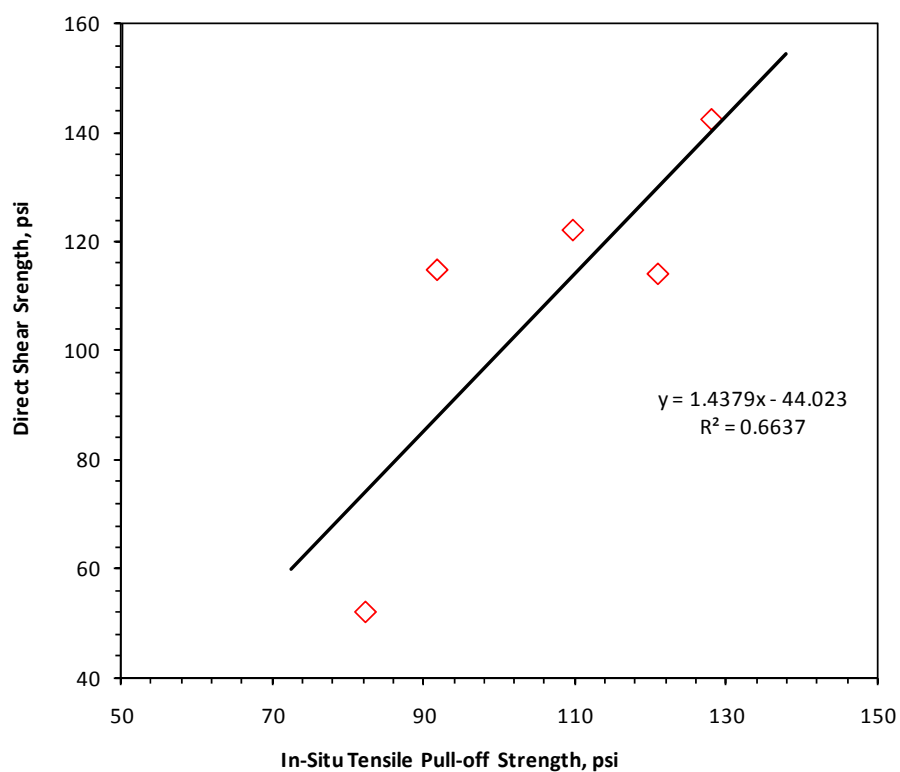


Figure 30. Correlation of Pull-Off Strength and Direct Shear Strength.

3.4 Simulated Aircraft Trafficking

Each of the replicates and treatments were subjected 1500 passes of simulated F-15E tire traffic using AFRL's F-15 load cart. Some environmental cracking (postulated to be shrinkage and/or thermal cracking) was observed prior to commencement of the trafficking experiment. However, during the conduct of the trafficking experiment, these cracks remained tight, and no FOD-creating distresses were observed.

3.5 Post-Trafficking In-Situ Pull-Off Experiments

The results of the post-trafficking in-situ pull-off experiments are tabulated in Table 5, and the data are summarized in the plot shown in Figure 31. For all treatments the pull-off strength was non-zero, indicating that the bond was not broken during the trafficking of the spall repairs. The highest post-trafficking in-situ bond strength was observed for the cold planer, with the other methods having bond strengths approximately one-half that of the cold planer. The P value matrix of the post-trafficking in-situ pull-off experiments is shown in Figure 32. The observed difference in mean value between the cold planer all the other four methods were statistically significant at the 95 percent confidence level.

Table 6. Post-Trafficking In-situ Pull-Off Data.

<i>Trial</i>	<i>Method</i>	<i>Spall Number</i>	<i>Replicate</i>	<i>Tensile Pull-off Strength, psi</i>
1	Cold Planer	1-1	1	20
2	Cold Planer	1-2	1	171
3	Cold Planer	1-2	2	370
4	Cold Planer	1-2	3	311
5	Cold Planer	1-2	4	286
6	Cold Planer	1-2	5	319
7	Cold Planer	1-3	1	166
8	Cold Planer	1-3	2	246
9	Cold Planer	1-3	3	202
10	Hydraulic Breaker	2-1	1	211
11	Hydraulic Breaker	2-1	2	136
12	Hydraulic Breaker	2-1	3	66
13	Hydraulic Breaker	2-1	4	193
14	Hydraulic Breaker	2-1	5	42
15	Hydraulic Breaker	2-1	6	292
16	Hydraulic Breaker	2-1	7	72
17	Hydraulic Breaker	2-1	8	134
18	Hydraulic Breaker	2-1	9	212
19	Hydraulic Breaker	2-1	10	91
20	Hydraulic Breaker	2-2	1	154
21	Hydraulic Breaker	2-2	2	70
22	Hydraulic Breaker	2-2	3	41
23	Hydraulic Breaker	2-2	4	139
24	Hydraulic Breaker	2-2	5	158

Table 6 (Continued). Post-Trafficking In-situ Pull-Off Data.

<i>Trial</i>	<i>Method</i>	<i>Spall Number</i>	<i>Replicate</i>	<i>Tensile Pull- off Strength, psi</i>
25	Hydraulic Breaker	2-3	1	66
26	Hydraulic Breaker	2-3	2	82
27	Jackhammer	3-1	1	212
28	Jackhammer	3-1	2	183
29	Jackhammer	3-1	3	48
30	Jackhammer	3-1	4	217
31	Jackhammer	3-2	1	169
32	Jackhammer	3-2	2	28
33	Jackhammer	3-2	3	154
34	Jackhammer	3-2	4	99
35	Jackhammer	3-2	5	50
36	Jackhammer	3-2	6	102
37	Jackhammer	3-2	7	338
38	Jackhammer	3-3	1	20
39	Jackhammer	3-3	2	122
40	Jackhammer	3-3	3	60
41	Jackhammer	3-3	4	121
42	Jackhammer	3-3	5	17
43	Jackhammer	3-3	6	63
44	Gang Saw (3/4 in.)	4-1	1	133
45	Gang Saw (3/4 in.)	4-1	2	181
46	Gang Saw (3/4 in.)	4-1	3	140
47	Gang Saw (3/4 in.)	4-1	4	202
48	Gang Saw (3/4 in.)	4-1	5	218
49	Gang Saw (3/4 in.)	4-1	6	52
50	Gang Saw (3/4 in.)	4-1	7	99
51	Gang Saw (3/4 in.)	4-1	8	130
52	Gang Saw (3/4 in.)	4-1	9	226
53	Gang Saw (3/4 in.)	4-1	10	165
54	Gang Saw (3/4 in.)	4-1	11	157
55	Gang Saw (3/4 in.)	4-2	1	184
56	Gang Saw (3/4 in.)	4-2	2	120
57	Gang Saw (3/4 in.)	4-2	3	216
58	Gang Saw (3/4 in.)	4-2	4	218
59	Gang Saw (3/4 in.)	4-2	5	164
60	Gang Saw (3/4 in.)	4-2	6	217
61	Gang Saw (3/4 in.)	4-3	1	63
62	Gang Saw (3/4 in.)	4-3	2	176
63	Gang Saw (3/4 in.)	4-3	3	93
64	Gang Saw (3/4 in.)	4-3	4	165
65	Gang Saw (3/4 in.)	4-3	5	116
66	Gang Saw (3/4 in.)	4-3	6	44
67	Gang Saw (3/4 in.)	4-3	7	157
68	Gang Saw (1-1/2 in.)	5-1	1	256

Table 6 (Concluded). Post-Trafficking In-situ Pull-Off Data.

<i>Trial</i>	<i>Method</i>	<i>Spall Number</i>	<i>Replicate</i>	<i>Tensile Pull- off Strength, psi</i>
69	Gang Saw (1-1/2 in.)	5-1	2	211
70	Gang Saw (1-1/2 in.)	5-1	3	113
71	Gang Saw (1-1/2 in.)	5-1	4	23
72	Gang Saw (1-1/2 in.)	5-1	5	130
73	Gang Saw (1-1/2 in.)	5-1	6	115
74	Gang Saw (1-1/2 in.)	5-1	7	57
75	Gang Saw (1-1/2 in.)	5-1	8	124
76	Gang Saw (1-1/2 in.)	5-1	9	162
77	Gang Saw (1-1/2 in.)	5-1	10	155
78	Gang Saw (1-1/2 in.)	5-1	11	186
79	Gang Saw (1-1/2 in.)	5-1	12	143
80	Gang Saw (1-1/2 in.)	5-2	1	194
81	Gang Saw (1-1/2 in.)	5-2	2	125
82	Gang Saw (1-1/2 in.)	5-2	3	217
83	Gang Saw (1-1/2 in.)	5-2	4	409
84	Gang Saw (1-1/2 in.)	5-2	5	163
85	Gang Saw (1-1/2 in.)	5-2	6	219
86	Gang Saw (1-1/2 in.)	5-2	7	230
87	Gang Saw (1-1/2 in.)	5-2	8	195
88	Gang Saw (1-1/2 in.)	5-2	9	64
89	Gang Saw (1-1/2 in.)	5-2	10	193
90	Gang Saw (1-1/2 in.)	5-3	1	125
91	Gang Saw (1-1/2 in.)	5-3	2	53
92	Gang Saw (1-1/2 in.)	5-3	3	146
93	Gang Saw (1-1/2 in.)	5-3	4	194
94	Gang Saw (1-1/2 in.)	5-3	5	106
95	Gang Saw (1-1/2 in.)	5-3	6	249
96	Gang Saw (1-1/2 in.)	5-3	7	23
97	Gang Saw (1-1/2 in.)	5-3	8	123
98	Gang Saw (1-1/2 in.)	5-3	9	40

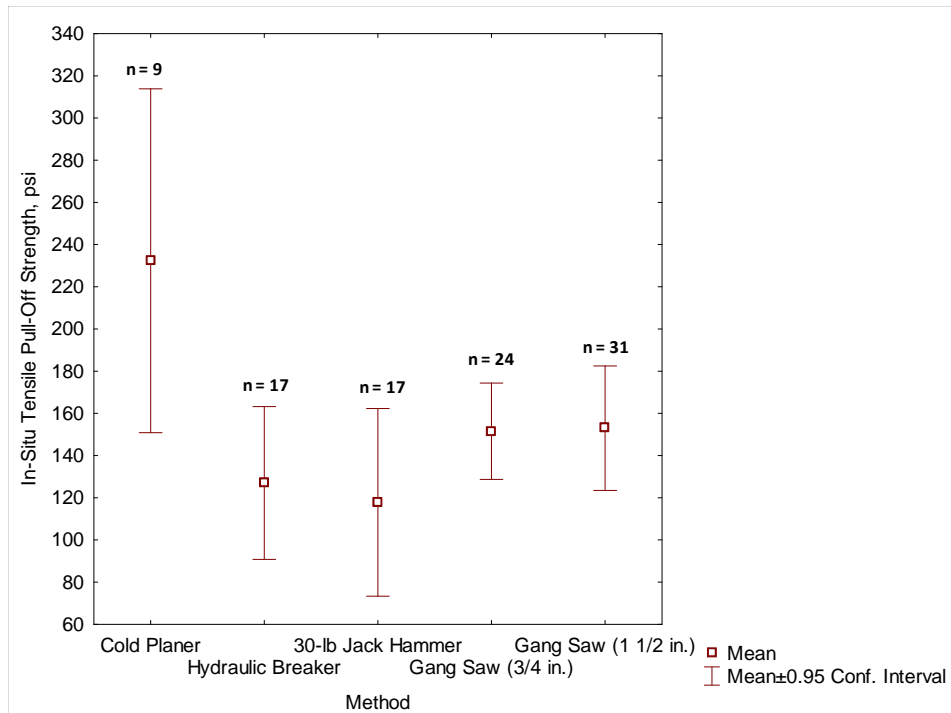


Figure 31. Whisker Plot of Post-Trafficking In-Situ Pull-Off Data.

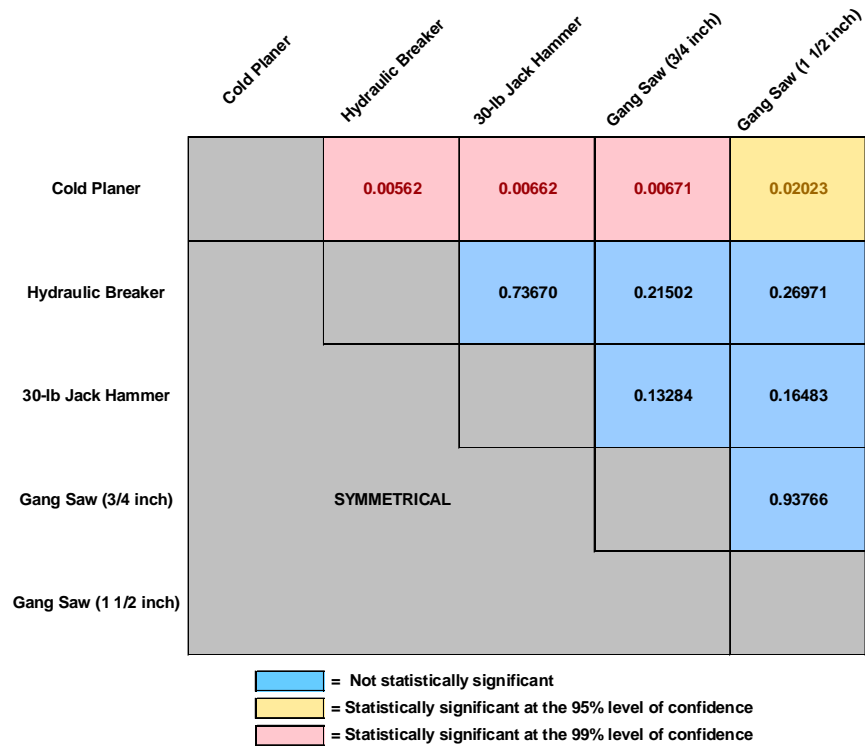


Figure 32. P Value Matrix for Post-Trafficking Direct Shear Experiments.

3.6 Post-Trafficking Direct Shear Experiments

The results of the post-trafficking direct shear experiments are tabulated in Table 7, and these results are summarized in the plot shown in Figure 33. The greatest observed mean pull-off strength was for the gang saw at $\frac{3}{4}$ inch spacing, followed, in order, by the gang saw at $1\frac{1}{2}$ inches spacing, jackhammer, cold planer, and finally the hydraulic breaker. However, as presented in Figure 34, only the hydraulic breaker was statistically significant.

Table 7. Post-Trafficking Direct Shear Data.

<i>Trial</i>	<i>Name</i>	<i>Spall Number</i>	<i>Replicate</i>	<i>Direct Shear Bond Strength, psi</i>
1	Cold Planer	1-1	1	167.91
2	Cold Planer	1-1	2	28.65
3	Cold Planer	1-1	3	302.79
4	Cold Planer	1-2	1	178.25
5	Cold Planer	1-2	2	150.80
6	Cold Planer	1-2	3	32.63
7	Cold Planer	1-2	4	230.38
8	Cold Planer	1-3	1	72.42
9	Cold Planer	1-3	2	81.96
10	Cold Planer	1-3	3	258.23
11	Cold Planer	1-3	4	90.32
12	Hydraulic Breaker	2-1	1	105.04
13	Hydraulic Breaker	2-1	2	79.18
14	Hydraulic Breaker	2-1	3	158.76
15	Hydraulic Breaker	2-1	4	104.25
16	Hydraulic Breaker	2-2	1	113.00
17	Hydraulic Breaker	2-2	2	228.79
18	Hydraulic Breaker	2-2	3	157.96
19	Hydraulic Breaker	2-2	4	113.80
20	Hydraulic Breaker	2-3	1	169.50
21	Hydraulic Breaker	2-3	2	185.81
22	Hydraulic Breaker	2-3	3	68.04
23	Hydraulic Breaker	2-3	4	136.87
24	30-lb Jackhammer	3-1	1	230.38
25	30-lb Jackhammer	3-1	2	159.95
26	30-lb Jackhammer	3-1	3	299.21
27	30-lb Jackhammer	3-1	4	275.74
28	30-lb Jackhammer	3-2	1	151.20
29	30-lb Jackhammer	3-3	2	268.57
30	30-lb Jackhammer	3-4	3	160.35
31	30-lb Jackhammer	3-3	1	144.43
32	30-lb Jackhammer	3-3	2	80.77
33	Gang Saw (3/4 inch)	4-1	1	134.09
34	Gang Saw (3/4 inch)	4-1	2	279.32
35	Gang Saw (3/4 inch)	4-1	3	207.30
36	Gang Saw (3/4 inch)	4-1	4	249.48

Table 7 (Concluded). Post-Trafficking Direct Shear Data.

<i>Trial</i>	<i>Name</i>	<i>Spall Number</i>	<i>Replicate</i>	<i>Direct Shear Bond Strength, psi</i>
37	Gang Saw (3/4 inch)	4-2	1	99.07
38	Gang Saw (3/4 inch)	4-2	2	263.00
39	Gang Saw (3/4 inch)	4-2	3	202.92
40	Gang Saw (3/4 inch)	4-3	1	224.41
41	Gang Saw (3/4 inch)	4-3	2	139.26
42	Gang Saw (3/4 inch)	4-3	3	216.45
43	Gang Saw (3/4 inch)	4-3	4	305.58
44	Gang Saw (1-1/2 inch)	5-1	1	220.43
45	Gang Saw (1-1/2 inch)	5-1	2	267.38
46	Gang Saw (1-1/2 inch)	5-1	3	315.92
47	Gang Saw (1-1/2 inch)	5-1	4	194.57
48	Gang Saw (1-1/2 inch)	5-2	1	229.18
49	Gang Saw (1-1/2 inch)	5-2	2	179.05
50	Gang Saw (1-1/2 inch)	5-2	3	206.50
51	Gang Saw (1-1/2 inch)	5-2	4	77.19
52	Gang Saw (1-1/2 inch)	5-3	1	116.58
53	Gang Saw (1-1/2 inch)	5-3	2	198.55
54	Gang Saw (1-1/2 inch)	5-3	3	194.17
55	Gang Saw (1-1/2 inch)	5-3	4	252.26

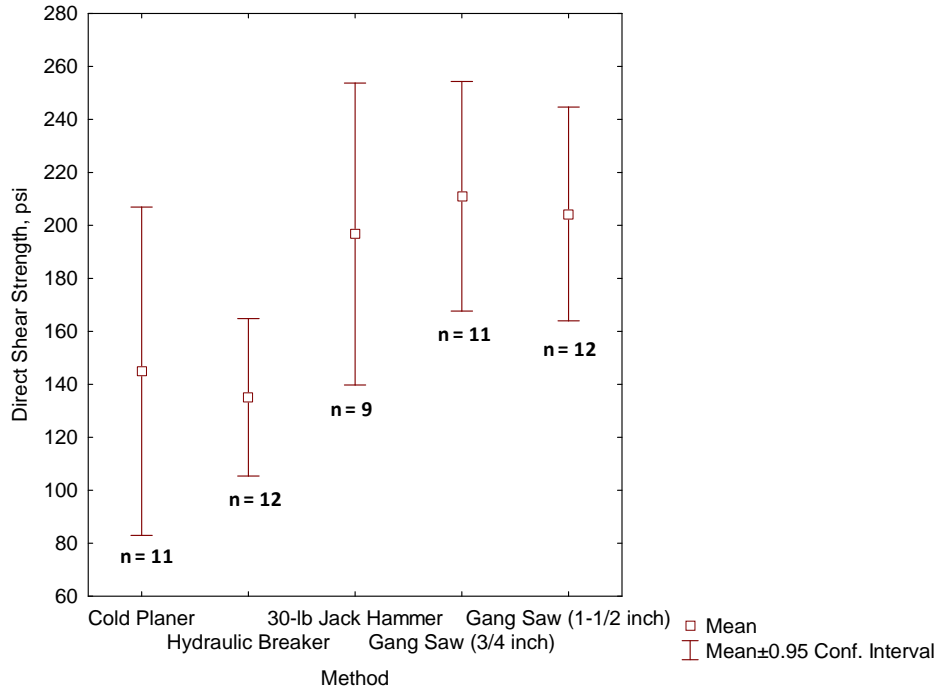


Figure 33. Whisker Plot of Post-Trafficking Direct Shear Data.

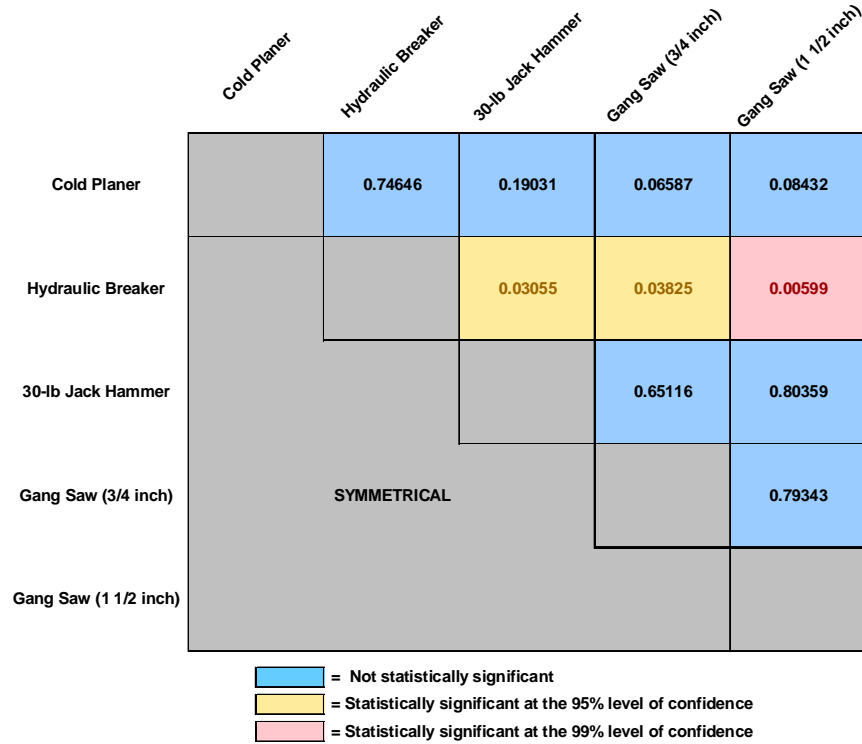


Figure 34. P Value Matrix for Post-Trafficking Direct Shear Experiments.

3.7 Petrographic Examination

3.7.1 Results

Figure 35 shows the two raw data sets collected from the immersion scanning system for the specimens in this study. These data were re-sampled so that both data sets had a y-axis spacing of 0.01 inch (or 100 scan lines per inch). From this figure one can observe a darkening or shift in the image panels from left to right. Figure 36 shows a second graphing made to try to quantify this observation. In Figure 36 each scanned line in the z-direction (vertical) was averaged; thus we are looking at the average change in z as we move across the samples in y. Note that the first and last panels are two different scans of the same panel (or specimen). From this data we can see that the primary difference is an offset between these two datasets. In Figure 37 and Figure 38 relative location and legends are given for each sample in the scanned groups. Note that specimen 070100 (the gang saw at $\frac{3}{4}$ inch spacing) was located in both glued up specimen sets to provide a comparison check between the two. Two different control specimens both labeled 070102 (core from pad) were also included in each scanned group

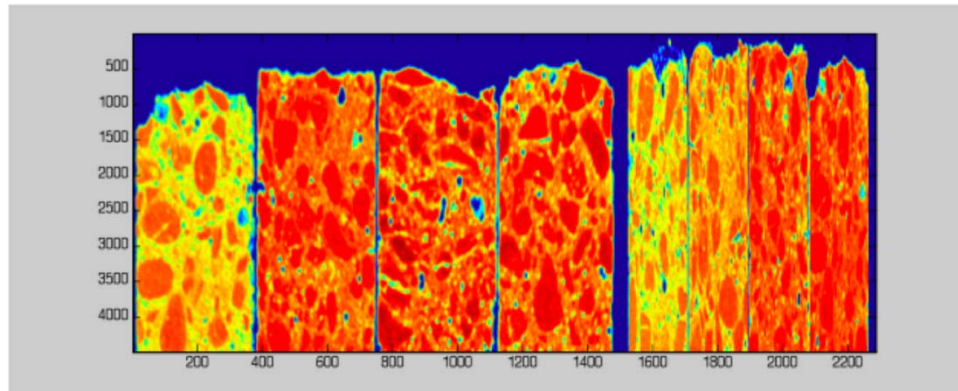


Figure 35. Raw Ultrasonic Reflection Image Data for Two Specimens Sets with One Duplicate Sample for Matching.

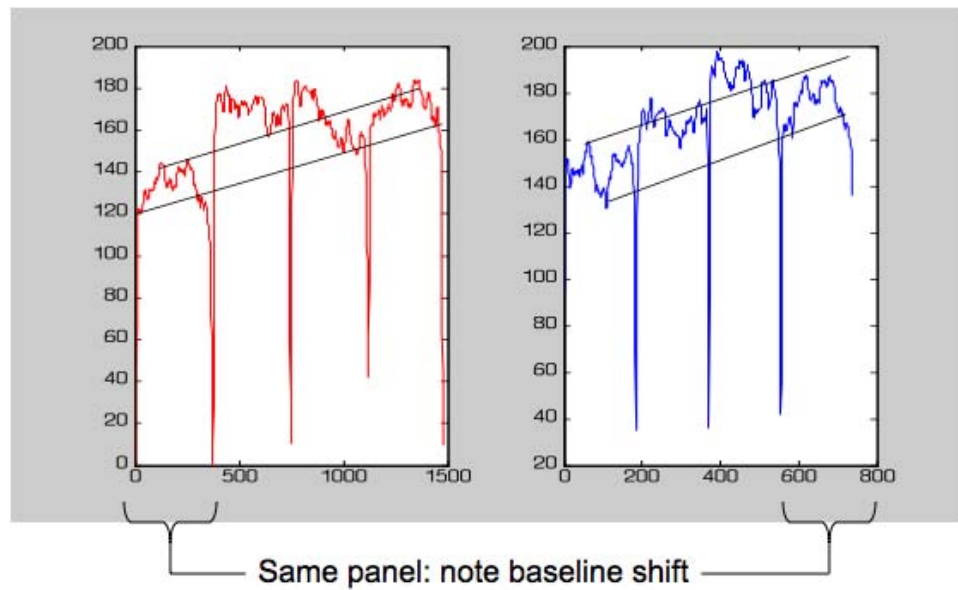


Figure 36. Averaged Data in Z across Two Data Sets.

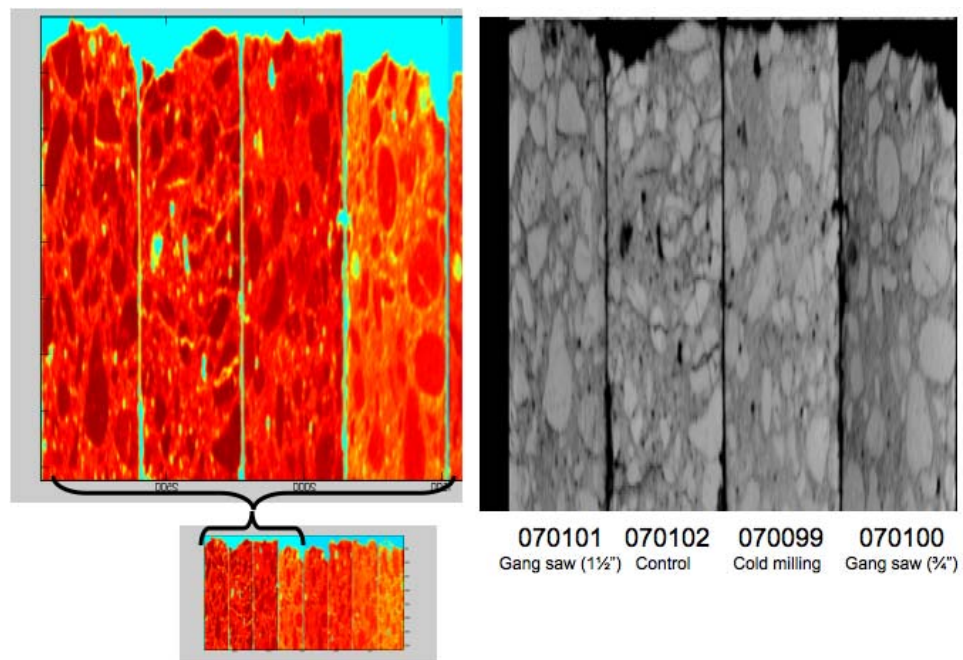


Figure 37. Color and Greyscale Images of First Group of Scanned Specimens.

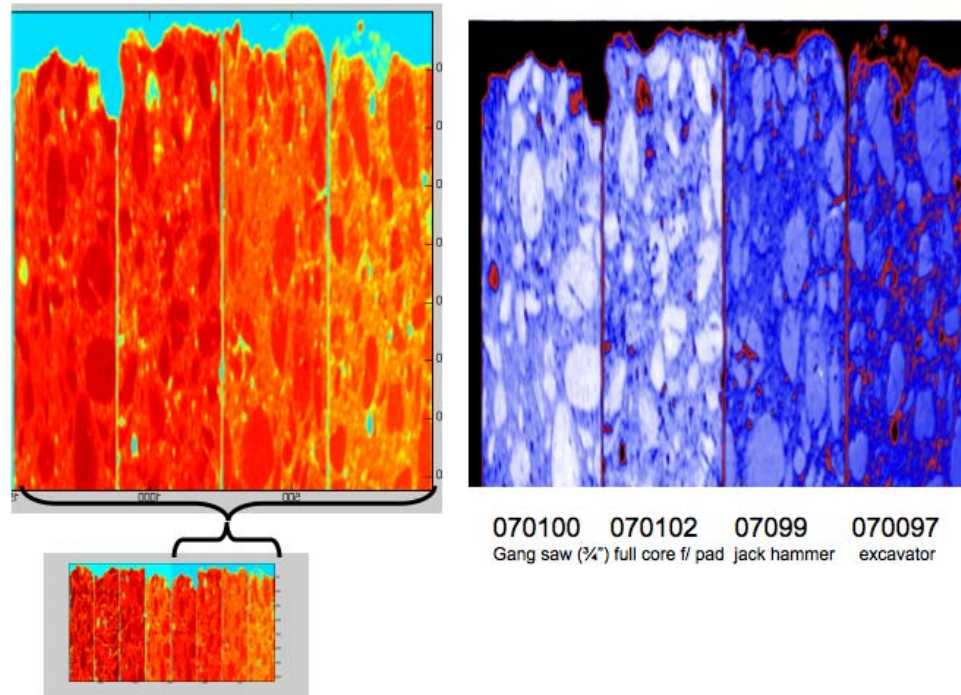


Figure 38. Color and Grayscale Images of the Second Group of Scanned Specimens.

Figure 39 shows an example of detected aggregate cracking and entrapped air. For each specimen the N value (starting palate value) was adjusted so that visual air voids were captured as accurately as possible. In general, specification of the N value picks the starting point of the Matlab HSV color palate. The value of N was determined by trial and error manual visual comparisons such that the color-coded image most accurately depicted the observable larger air voids. The equation used to adjust the palate is shown in Figure 39.

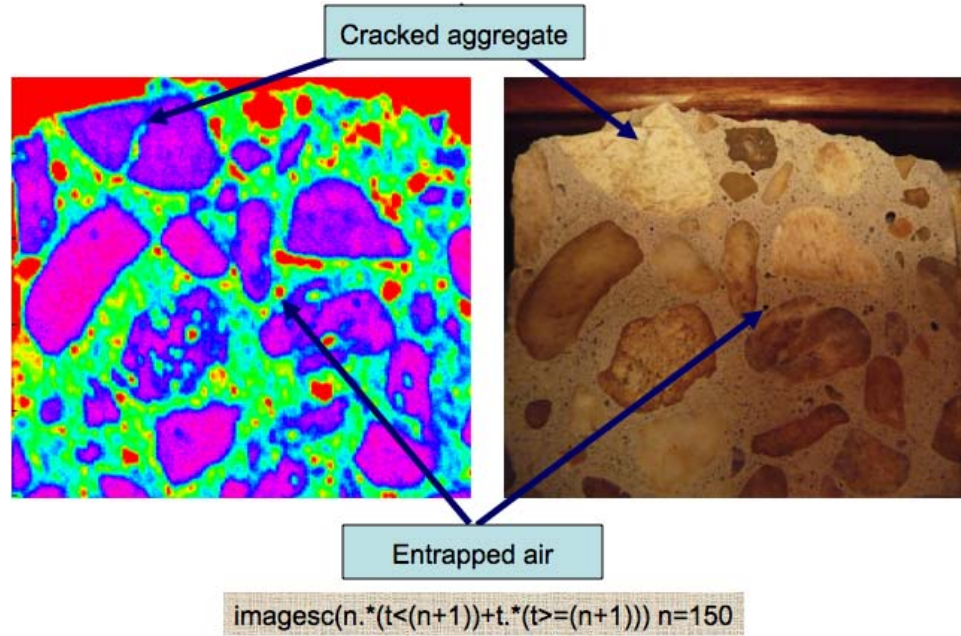


Figure 39. Adjustment of Ultrasonic Color Palate to Enhance Features.

Table 8 gives the figure and specimen relationship for each scanned panel. In Figure 39 through Figure 46 each adjusted scan is shown alongside a corresponding digital photograph.

Table 8. Figure and Specimen Relationship.

<i>Image Location</i>	<i>Control Number</i>	<i>Descriptions</i>	<i>N</i>
Figure 40	70102	Control	165
Figure 41	70102	Full core from test pad	150
Figure 42	70101	Gang saw (1½-inch spacing)	150
Figure 43	70100	Gang Saw (¾-inch spacing)	24/29
Figure 44	7099	Cold planer	160
Figure 45	7099	Jackhammer	130
Figure 46	7097	Hydraulic breaker	120

3.7.2 Analysis of Results

In Figure 43 the results from the twice-scanned sample “Gang Saw (¾-inch) 070100” show good agreement once palate corrections are made. In Figure 45 some of the weak (low density or low mechanical impedance) aggregates are indicated in the photograph. In general the percentage of weak aggregate seen appeared to be within the observed rate in prior experiments. In the control core scans, particularly in Figure 41 a number of small cracks are seen. In some cases these appear initiate at or are related to intrinsically cracked aggregate. The only damage observed to significantly penetrate the surface is the zoomed in

photographic view shown in Figure 46 (hydraulic breaker). The large aggregates near the surface are highly cracked; however, these cracks seem consistent with others observed, such as in Figure 40 and Figure 41.

From an examination of these data, only the hydraulic breaker produced significant subsurface damage of the rock or paste at depths of up to ½ inch.

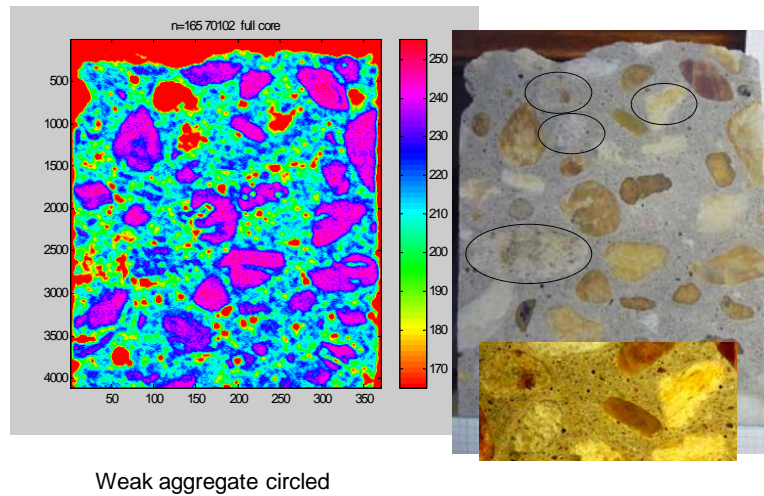


Figure 40. Images of Control Core.

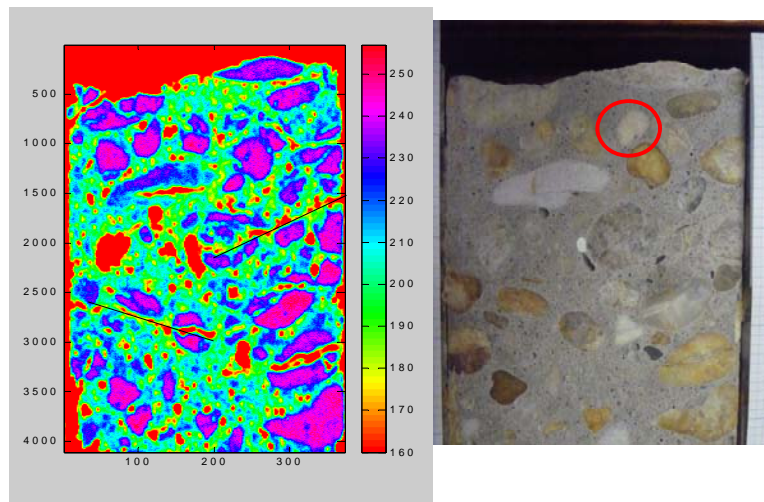


Figure 41. Images of Full Core from Pad.

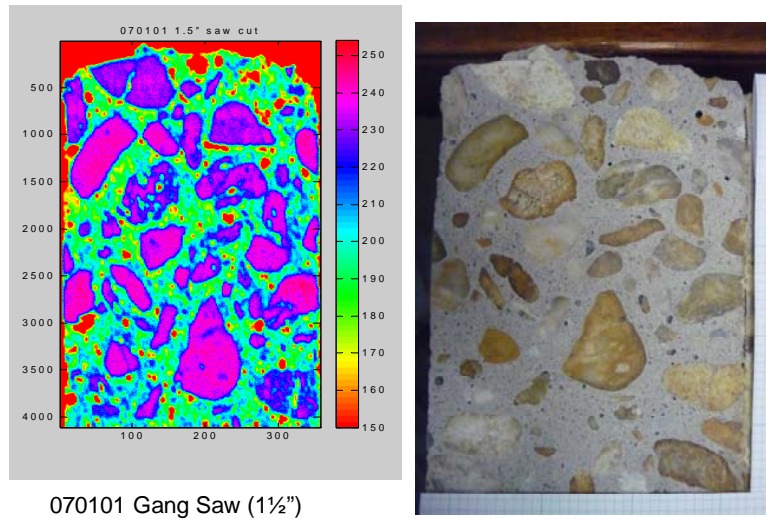


Figure 42. Images of Core from Gang Saw (1½-inch Spacing).

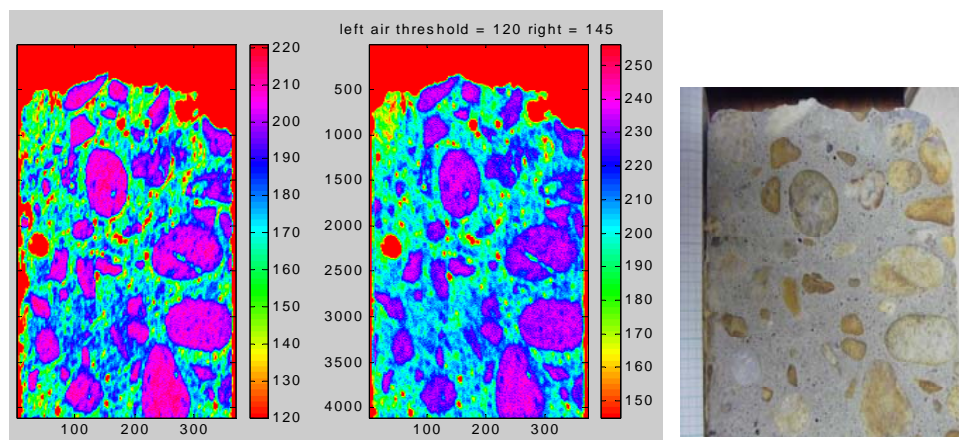


Figure 43. Images of Core from Gang Saw (3/4-inch Spacing).

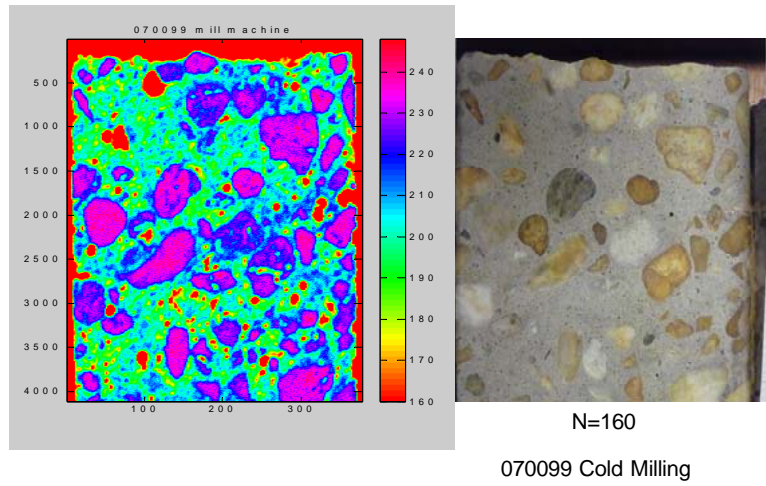


Figure 44. Images of Core from Cold Planer.

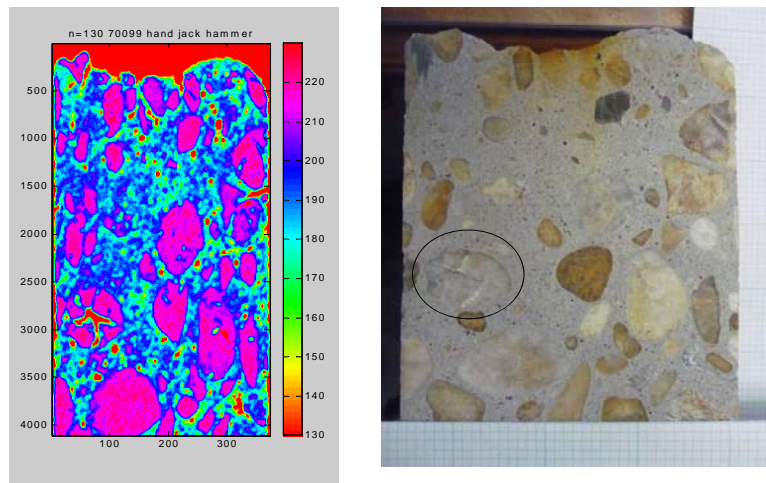


Figure 45. Images of Core from Jackhammer.

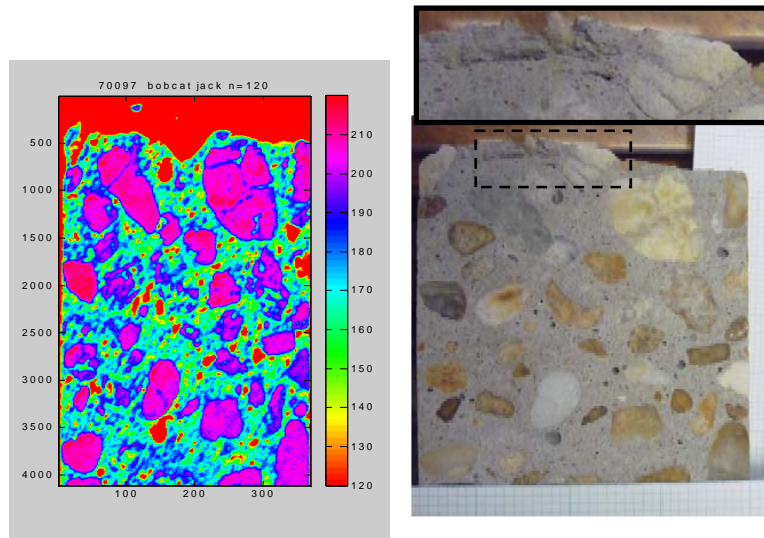


Figure 46. Images of Core from Hydraulic Breaker.

3.8 Summary of Significant Results

3.8.1 Production Rate

1. Each of the methods tested had a significant improvement in production rate over the 30-pound jackhammer.
2. The most efficient method was the cold planer, which, on average, was approximately 58 percent more efficient than the jackhammer. It was the only method investigated expected to consistently meet the research objective of excavating a nominal 2 foot square by 4-inch deep spall in 15 minutes or less.
3. The second most efficient method was the multiple blade (gang) saw. The 1½-inch blade spacing was significantly more efficient than the ¾-inch blade spacing.
4. The hydraulic breaker (excavator) was more efficient than the control case (manual jackhammer), but it causes significant damage to the upper ½-inch or so of the substrate materials.

3.8.2 Bond Strength

1. Pre-traffic bond strength data (in-situ direct tension tests and direct shear tests) indicated that only the hydraulic breaker had a significantly lower bond strength prior to trafficking with 1500 passes of simulated F-15 load.
2. The post-trafficking bond strength data indicated that the cold planer method resulted in significantly greater bond strength after 1500 passes of simulated F-15 traffic. This is evidence of significantly greater performance for this method of preparing a spall for placement of rapid setting material.

3.8.3 Petrographic Examination

1. Petrographic examinations indicated that none of the methods investigated produced any significant damage of the aggregate or paste below the surface with the exception of the hydraulic breaker, which produced cracking the matrix and fractured aggregates up to ½ inch below the top surface.

3.8.4 Performance under Traffic

1. Each of the replicates and treatments were subjected to 1,500 passes of simulated F-15E traffic. During the conduct of the testing, no cracking, spalling, or any other type FOD-creating distresses were observed.
2. Some environmental cracking (postulated to be shrinkage and/or thermal cracking) was observed prior to commencement of the trafficking experiment. However, during the conduct of the trafficking experiment, these cracks remained tight, and no FOD-creating distresses were observed.

4 Conclusions and Recommendations

4.1 Conclusions

4.1.1 Excavation Methods

Five excavation methods (treatments) were used to prepare a nominal 2-foot-wide 2-foot-long by 4-inch-deep spalls:

1. Saw cut and 30-pound jackhammer (baseline or current standard),
2. Saw cut and a hydraulic breaker on a skid steer tractor,
3. Multiple-blade gang saw with saw spacing at $\frac{3}{4}$ inch,
4. Multiple-blade gang saw with saw spacing at $1\frac{1}{2}$ inches, and
5. Cold planer attachment for a skid steer loader.

The control case was the 30-pound jackhammer. Each of the four methods tested had a significant improvement in production rate over the 30-pound jackhammer. The most efficient method was the cold planer, which, on average, was approximately 58 percent more efficient than the jackhammer. The second most efficient method was the gang saw at $1\frac{1}{2}$ inch spacing, followed by the hydraulic breaker, followed by gang saw with spacing at $\frac{3}{4}$ inch spacing. Only the cold planer can meet the requirement of being able to excavate 2-foot square by 4-inch deep spall in no more than 15 minutes.

4.1.2 Simulated Aircraft Trafficking

Each of the replicates and treatments were subjected to 1,500 passes of simulated F-15E. During the conduct of the testing, no load-related cracking, spalling, or any other type FOD-creating distresses were observed.

4.1.3 In-Situ Bond Strength

In-situ bond tests were performed both prior to and after simulated aircraft trafficking. Pre-trafficking, the greatest observed mean pull-off strength was for the cold planer, followed, in order, by the jackhammer, gang saw at $1\frac{1}{2}$ inches spacing, gang saw at $\frac{3}{4}$ inch spacing, and finally the hydraulic breaker. However, only the differences in the means between the hydraulic breaker and cold planer and hydraulic breaker and jackhammer were statistically significant at the 95 percent confidence level, and one cannot statistically distinguish between the means of the other treatments at the 95 percent confidence level.

The highest post-trafficking in-situ bond strength was observed for the cold planer, with the other methods having bond strengths approximately one-half that of the cold planer. The observed difference in mean value between the cold planer

all the other four methods were statistically significant at the 95 percent confidence level.

4.1.4 Direct Shear Strength

Analysis of the correlation between the in-situ tensile pull-off strength and the direct shear strength experiments indicated that the two metrics of bond strength are positively correlated with a correlation coefficient (R^2) of 0.66. However, the statistical significance of the direct shear strength results was not as powerful as those of the in-situ direct pull off strengths. Because the direct shear strength test is not an accepted test method per ASTM, it was concluded that the results of the direct shear strength tests should not be used to draw conclusions concerning the efficacy of the methods until further development and analysis of this methodology is conducted.

4.1.5 Petrographic Examination

Petrographic examinations indicated that only the hydraulic breaker produced significant subsurface damage of the rock or paste at depths of up to ½ inch.

4.2 Recommendations

The cold planer method should be adopted as a standard method of preparing spalls for placement of a rapid-setting spall repair material. The cold planer equipment can be purchased as an attachment to skid-steer loader. While the time to prepare a spall depends upon the characteristics of the spall and the skill of the operating, use of this equipment requires about half the time to prepare the spall as compared to the control case of a manual jackhammer. The cold planer equipment, under the control of an experienced operator, can prepare a two foot square by 4 inch deep spall for placement of rapid-setting material in less than 15 minutes. Furthermore, spalls prepared with this method retain superior bond strength after aircraft trafficking and are expected to provide superior performance compared to those prepared with other conventional and experimental methods evaluated in the study.

5 References

1. Speer, Benjamin S. *A Value-Focused Thinking Model for the Selection of the Best Rigid Pavement Partial-Depth Spall Repair Material*, AFIT/GEM/ENS-07-4, Air Force Institute of Technology, Wright-Patterson Air Force Base, OH, March 2007.
2. Department of the Air Force. *Spall Repair of Portland Cement Concrete (PCC) Airfield Pavements in Expeditionary Environments*, ETL 07-8, Air Force Civil Engineer Support Agency, Tyndall AFB, FL, 27 Jul 2007.
3. The American Concrete Institute. "Guide for the Selection of Materials for the Repair of Concrete." ACI 546.3R-06, Farmington Hills, Michigan, December 2006.
4. Emmons, Peter. *Field Guide to Concrete Repair Application Procedures: Spall Repair of Horizontal Concrete Surfaces*, ACI RAP Bulletin 7, American Concrete Institute, 2005.
5. International Concrete Repair Institute. *Guide to Using In-Situ Tensile Pull-Off Tests to Evaluate Bond of Concrete Surface Materials*, Guideline No. 03739, International Concrete Repair Institute, Des Plaines, IL, March 2004.
6. ASTM. "Standard Test Method for Pull-Off Strength of Coatings Using Portable Adhesion Testers," ASTM D4541-2, ASTM International, West Conshohocken, PA., 2007.